Ecological Indicators 131 (2021) 108122

Contents lists available at ScienceDirect

Ecological Indicators

journal homepage: www.elsevier.com/locate/ecolind

Original Articles

# Ecology of peatland testate amoebae in Svalbard and the development of transfer functions for reconstructing past water-table depth and pH

Thomas G. Sim [a,*], Graeme T. Swindles [b,c], Paul J. Morris [a], Andy J. Baird [a], Dan J. Charman [d], Matthew J. Amesbury [d], Dave Beilman [e], Alex Channon [d], Angela V. Gallego-Sala [d]

[a] School of Geography, University of Leeds, Leeds, UK
[b] Geography, School of Natural and Built Environment, Queen's University Belfast, Belfast, UK
[c] Ottawa-Carleton Geoscience Centre and Department of Earth Sciences, Carleton University, Ottawa, Ontario, Canada
[d] Geography, College of Life and Environmental Sciences, University of Exeter, Exeter, UK
[e] Department of Geography and Environment, University of Hawaii Manoa, Honolulu, USA

ARTICLE INFO

*Keywords:*
Testate amoebae
Transfer function
High Arctic
Palaeohydrology
Ecology
Trophic gradient
Peatlands
Permafrost

ABSTRACT

Peatlands are valuable archives of information about past environmental conditions and represent a globally-important carbon store. Robust proxy methods are required to reconstruct past ecohydrological dynamics in high-latitude peatlands to improve our understanding of change in these carbon-rich ecosystems. The High Arctic peatlands in Svalbard are at the northern limit of current peatland distribution and have experienced rapidly rising temperatures of 0.81 °C per decade since 1958. We examine the ecology of peatland testate amoebae in surface vegetation samples from permafrost peatlands on Spitsbergen, the largest island of the Svalbard archipelago, and develop new transfer functions to reconstruct water-table depth (WTD) and pH that can be applied to understand past peatland ecosystem dynamics in response to climate change. These transfer functions are the first of their kind for peatlands in Svalbard and the northernmost developed to date. Multivariate statistical analysis shows that WTD and pore water pH are the dominant controls on testate amoeba species distribution. This finding is consistent with results from peatlands in lower latitudes with regard to WTD and supports work showing that when samples are taken across a long enough trophic gradient, peatland trophic status is an important control on the distribution of testate amoebae. No differences were found between transfer functions including and excluding the taxa with weak idiosomic tests (WISTs) that are most susceptible to decay. The final models for application to fossil samples therefore excluded these taxa. The WTD transfer function demonstrates the best performance ($R^2_{LOO}$ = 0.719, $RMSEP_{LOO}$ = 3.2 cm), but the pH transfer function also performs well ($R^2_{LOO}$ = 0.690, $RMSEP_{LOO}$ = 0.320). The transfer functions were applied to a core from western Spitsbergen and suggest drying conditions ~1750 CE, followed by a trend of recent wetting and increasing pH from ~1920 CE. These new transfer functions allow the reconstruction of past peatland WTD and pH in Svalbard, thereby enabling a greater understanding of long-term ecohydrological dynamics in these rapidly changing ecosystems.

## 1. Introduction

Peatlands and wetlands are widespread across the non-glaciated areas of the High Artic (Walker et al., 2005) and represent a substantial carbon store, with soils holding an estimated 34 ± 16 Pg C (Hugelius et al., 2014). High-latitude regions in general are now warming at two to three times the global average rate (Masson-Delmotte et al., 2018) and High Arctic areas are especially vulnerable to Arctic amplification feedbacks (Serreze and Barry, 2011). There are growing concerns that warming temperatures will expose greater amounts of soil carbon to decomposition via deeper permafrost thaw and that warming will increase rates of microbial decomposition, leading to a positive feedback with climate (Koven et al., 2015; Schuur et al., 2015). Conversely, increases in productivity associated with longer and warmer growing seasons may result in greater carbon accumulation in peatlands at mid-latitudes and in particular at high-latitudes (Gallego-Sala et al., 2018). Hydrological conditions are likely to be crucial factors influencing the balance of decomposition and productivity in peatlands, with excessive

* Corresponding author.
*E-mail address:* gy12tgs@leeds.ac.uk (T.G. Sim).

https://doi.org/10.1016/j.ecolind.2021.108122
Received 11 June 2021; Received in revised form 16 August 2021; Accepted 17 August 2021
Available online 30 August 2021

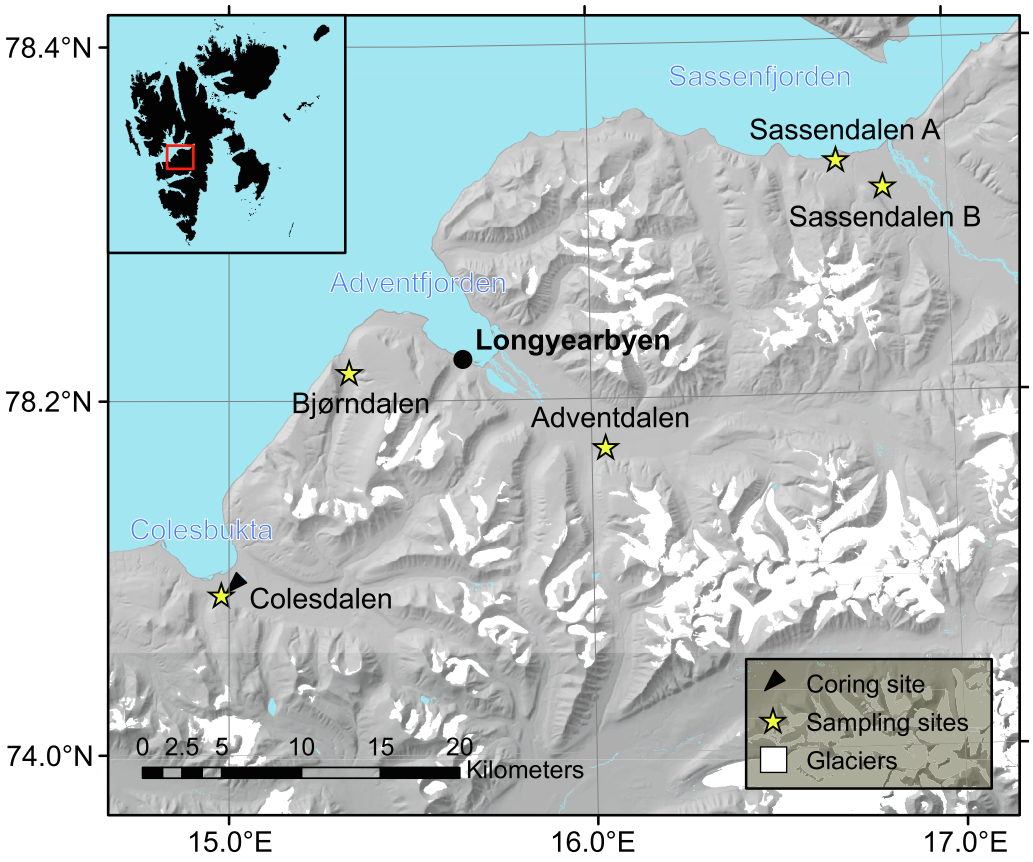


**Fig. 1.** Site map showing locations for surface sampling and the coring site, alongside glacier coverage. Digital elevation model data and glacier coverage sourced from the Norwegian Polar Institute (2014a, 2014b).

drying linked to increased $CO_2$ production from aerobic decomposition and inundation associated with elevated $CH_4$ production and flux to the atmosphere (Evans et al., 2021; Lawrence et al., 2015; Olefeldt et al., 2013). Nonetheless, comparatively less is known about High Arctic peatland processes compared with those in Boreal and Subarctic regions. Improved understanding of autogenic factors relating to permafrost thaw, hydrological change, productivity and decomposition are crucial for better quantifying future peatland carbon dynamics (Sim et al., 2021; Waddington et al., 2015). It is therefore important that proxy methods for reconstructing past ecohydrological dynamics in High Arctic peatlands are developed and rigorously tested to increase understanding of ecosystem change and to inform future predictions.

Testate amoebae are single-celled protists found on the surface of peatlands and are routinely used as palaeoenvironmental indicators because of the rapid response they demonstrate to hydrological conditions and the resistance they show to decomposition (Booth et al., 2010; Charman et al., 2000). Transfer functions to reconstruct past hydrological conditions have been developed for a range of regions and peatland types (e.g. Amesbury et al., 2018, 2016; Charman et al., 2007; Qin et al., 2021). More specifically, a number of transfer functions have now been developed in discontinuous (Lamarre et al., 2013; Swindles et al., 2015; Zhang et al., 2017) and continuous (Taylor et al., 2019a) permafrost peatlands. Taylor et al. (2019a) also developed a transfer function for electrical conductivity as a proxy for trophic status. In addition, certain species with weak idiosomic tests (WISTs) preserve less well (Payne, 2007; Swindles and Roe, 2007). This differential preservation needs to be considered by researchers because it can introduce taphonomic bias into transfer function reconstructions when WISTs are present in high abundance (Swindles et al., 2020).

Species diversity of testate amoebae is lower in High Arctic communities than lower latitude regions and there is thought to be a degree of regionalised distribution in taxa (Beyens and Bobrov, 2016). Previous studies have recorded the presence of testate amoebae in the contemporary and fossil records across the High Arctic (Beyens and Chardez, 1995; Sim et al., 2019) and specifically in Svalbard (Balik, 1994; Beyens et al., 1986c, 1986b, 1986a; Beyens and Chardez, 1987). However, the potential to use testate amoebae to reconstruct past hydrological conditions and/or trophic status for High Arctic peatlands with the development of transfer functions has yet to be fully explored.

In this paper we:

i. Examine the contemporary ecology of testate amoebae in continuous permafrost peatlands in Svalbard.
ii. Test the hypothesis that the contemporary distribution of testate amoeba species in Svalbard is primarily controlled by hydrological conditions.
iii. Develop transfer functions that can be used to reconstruct the most important controls on testate amoeba distribution.
iv. Examine the influence of excluding taxa with weak idiosomic tests (WISTs) on transfer function performance.
v. Apply the transfer function(s) to an independent subfossil testate amoeba record from a peat profile in Svalbard.

## 2. Study region

Svalbard is a Norwegian archipelago in the Arctic Ocean between 74°N and 81°N, of which the largest island of Spitsbergen is our study region. The climate is moderated by the West Spitsbergen Current (Walczowski and Piechura, 2011). It is therefore considerably warmer than comparable latitudes in Canada and Russia, with a mean annual

**Table 1**
Site overview and environmental conditions. Coordinates are averaged for all surface samples taken at each site. Negative WTD values means surface inundation.

| Site | Latitude (°N) | Longitude (°E) | Altitudinal range (m) | WTD range (cm) | MC range (%) | pH range | EC range (μS cm$^{-1}$) |
|---|---|---|---|---|---|---|---|
| Colesdalen | 78.09099 | 14.97843 | 47–51 | −2 to 22 | 60.1–95.8 | 5.15–6.75 | 108–360 |
| Sassendalen A | 78.33262 | 16.69365 | 11–14 | −3 to 22 | 80.6–97.1 | 6.49–7.03 | 249–519 |
| Sassendalen B | 78.31682 | 16.82241 | 16–20 | −1 to 34 | 63.7–89.1 | 6.72–8.22 | 237–1088 |
| Bjorndalen | 78.21644 | 15.33184 | 50–226 | 3 to23 | 80.2–92.7 | 5.24–6.48 | 83–344 |
| Adventdalen | 78.17288 | 16.03754 | 27–28 | −2 to 15 | 74.4–95.0 | 6.18–7.12 | 561–790 |

temperature of −4.6 °C (averaging period 1981–2010) at Svalbard Airport near Longyearbyen (78.25°N, 15.47°E, 28 m above sea level; Førland et al., 2011). Records for mean annual precipitation vary on a local scale with a mean annual precipitation (averaging period 1971–2000) of 196 mm at Svalbard Airport and 409 mm ~108 km north northwest at Ny-Ålesund (Hanssen-Bauer et al., 2019). Reanalysis temperature and precipitation data suggests our predominantly low-altitude sampling sites (Fig. 1; Table 1) are likely to experience similar climatic conditions to those at Svalbard Airport (Vikhamar Schuler and Østby, 2020). Ice-free areas in Svalbard are characterised by tundra with vegetation types including sedge, grass and brown-moss wetlands and dwarf-shrub and herbs (Walker et al., 2005). Soil cover in Svalbard is estimated to be around 10% with the majority of the landscape cover being ice (70%) or exposed rock (20%) (Hugelius et al., 2013). Despite this limited soil cover, ~5% of the land area of Svalbard (equivalent to ~50% of total soil cover) is estimated to be accumulating peat (Tanneberger et al., 2017) and long-term carbon accumulation rates of 9–19.2 g m$^{-2}$ yr$^{-1}$ have been recorded (Nakatsubo et al., 2015).

Composite temperature data from Svalbard Airport between 1899 and 2017 show a linear increase of 3.1 °C per century despite cooler periods in the 1910s and 1960s, while reanalysis data for the whole of Svalbard show warming of 0.81 °C per decade from 1958 to 2017 (Hanssen-Bauer et al., 2019; Vikhamar Schuler and Østby, 2020). Furthermore, ice-core temperature reconstructions suggest twentieth century warming is the greatest experienced in the past 600 years (Isaksson et al., 2003). The rapid nature of recent warming makes Svalbard an interesting area to study recent changes in peatland vegetation, hydrology and carbon dynamics. Moreover, under medium to high greenhouse gas emission scenarios the future climate of Svalbard (1971–2000 to 2071–2100) is projected to show an increase of 7–10 °C in median annual temperature and a 45–65% increase in median annual precipitation (Hanssen-Bauer et al., 2019), potentially creating more favourable conditions for peat formation.

Scientists have studied testate amoebae in Svalbard since as early as the ninetieth century (Ehrenberg, 1870; Scourfield, 1897). Since then, pioneering researchers have investigated testate amoebae in a largely exploratory and descriptive manner (Awerinzew, 1907; Balik, 1994; Bonnet, 1965; Opravilova, 1989; Penard, 1903; Schönborn, 1966). More ecology-focused research in the 1980s found moisture content to be a key control on species distribution in lichens and mosses on Northwest Spitsbergen, with notable taxa including: *Corythion dubium*, *Centropyxis aerophila*, *Trinema lineare*, *Assulina muscorum*, *Phryganella acropodia* and *Euglypha rotunda* (Beyens et al., 1986c). In aquatic environments on Northwest Spitsbergen, *C. aerophila* and *Paraquadrula irregularis* were the most common species observed, with the former associated with more acid waters and the latter more alkaline (Beyens et al., 1986b). Additionally, samples from mosses and pools on Edgeøya documented the first occurrence on the Svalbard archipelago of the predominantly Arctic taxon *Conicocassis pontigulaformis* (Beyens et al., 1986a). Changes in local hydrological conditions between ~5000 and 3800 BP have been inferred from testate amoeba preserved in peat layers on Edgeøya (Beyens and Chardez, 1987); however, the number of testate amoebae counted were extremely low and no statistical transfer function was used. More recent ecological work in Svalbard (Mazei et al., 2018) suggests a reduced abundance of *P. acropodia* and *C. aerophila* in soils enriched with guano, tentatively linked with changing nutrient supply and the availability of fungal food sources.

## 3. Method

### 3.1. Sampling

In August 2019 we collected 103 surface vegetation samples from five permafrost peatland areas in Svalbard, encompassing a representative range of environmental conditions (Fig. 1 and Table 1). Surface vegetation samples mainly comprised bryophytes, but also included sedges such as *Eriophorum* spp. and *Carex* spp. in hummock areas. Around 70% of Svalbard is covered by glaciers or permanent ice (Hugelius et al., 2013); therefore our study sampled a representative range of environments from the main ice-free area in Svalbard. The geology of the study region is predominantly characterised by the sandstones, siltstones and shales of the Central Tertiary Basin of Svalbard, with a shift to a limestone and dolostone bedrock towards the east in Sassendalen (Elvevold et al., 2007). Water-table depth (WTD) was determined by augering a well and measuring the water-table at regular intervals until it had stabilised. Both pH and electrical conductivity (EC) of the pore water in each augered well were measured using calibrated field meters. A peat core was extracted from a permafrost peatland of approximately 0.25 km$^2$ located on the valley floor towards the southern margin of the U-shaped valley of Colesdalen, Svalbard (78.09131°N, 14.98783°E). Analysis of this core provided a palaeo dataset of subfossil testate amoebae upon which to apply transfer functions. The core was sampled from a lawn area where the surface vegetation was characterised by Cyperaceae and brown mosses, including *Tomentypnum nitens* and *Aulacomnium palustre*. The core was extracted using a box corer to the base of the active layer (45 cm) and with a permafrost drill corer down to 91 cm.

### 3.2. Surface vegetation and peat properties

From the surface vegetation samples, ~5 g of material for each sample was weighed, dried overnight at 105 °C and then reweighted to calculate gravimetric moisture content (MC) (Chambers et al., 2011). The Colesdalen core was sub-sampled into 1-cm slices and measurements were made of dry bulk density, loss-on-ignition (LOI) and concentrations of carbon (C) and nitrogen (N). Dry bulk density (g cm$^{-3}$) was calculated by dividing dry mass of peat (g; dried overnight at 105 °C) by the total sample volume (cm$^3$), while LOI (%) was calculated by subtracting ash mass (g; after 8 h in a 550 °C furnace) from dry mass (g), before dividing this by dry mass and multiplying the product by 100 (Chambers et al., 2011). C and N contents were measured on a ThermoScientific Flash (2000) Series CHNS/O analyser.

### 3.3. Age-depth modelling

The chronology of the Colesdalen peat profile was determined using $^{210}$Pb and $^{14}$C dating methods. The $^{14}$C dates ($n = 3$) were analysed from above ground plant macrofossils on a 3MV accelerator mass spectrometer (AMS) at the André E. Lalonde AMS Laboratory, University of Ottawa, Canada (Supplementary Table 1). The dates were calibrated using the IntCal20 calibration curve (Reimer et al., 2020) and an age-depth profile (Supplementary Fig. 1) was constructed using the R

**Table 2**
Overview of 60 testate amoebae taxa identified, type (testate amoeba = TA; taxa with weak idiosomic tests = WIST), number, max abundance and authority.

| Taxon | Type | Code | In n samples | Max (%) | Authority |
|---|---|---|---|---|---|
| *Alabasta militaris* | TA | ALMI | 2 | 0.6 | Penard 1890; Duckert, Blandenier, Kosakyan and Singer 2018 |
| *Arcella arenania* | TA | ARAR | 8 | 5.5 | Greef 1866 |
| *Arcella catinus* | TA | ARCA | 34 | 24.4 | Penard 1890 |
| *Arcella discoides* | TA | ARDI | 49 | 46.6 | Ehrenberg 1843 |
| *Arcella hemisphaerica* | TA | ARHE | 13 | 10.5 | Perty 1852 |
| *Archerella flavum* | TA | ARFL | 23 | 45.4 | Archer 1877; Loeblich and Tappan 1961 |
| *Assulina muscorum* | TA | ASMU | 35 | 35.6 | Greeff 1888 |
| *Assulina scandinavica* | TA | ASSC | 3 | 1.4 | Penard 1890 |
| *Bullinularia indica* | TA | BUIN | 1 | 1.7 | Penard 1907 |
| *Campascus minutus* | TA | CAMI | 32 | 67.0 | Penard 1902 |
| *Centropyxis aculeata* | TA | CEAC | 6 | 3.7 | Ehrenberg 1838 |
| *Centropyxis aerophila* | TA | CEAE | 95 | 59.3 | Deflandre 1929 |
| *Centropyxis constricta* | TA | CECO | 26 | 7.1 | Ehrenberg 1841; Penard 1890 |
| *Centropyxis gasparella* | TA | CEGA | 5 | 2.8 | Chardez, Beyens and De Bock 1988 |
| *Centropyxis orbicularis* | TA | CEOR | 9 | 3.7 | Deflandre 1929 |
| *Centropyxis plagiostoma* | TA | CEPLAG | 11 | 1.6 | Bonnet and Thomas 1955 |
| *Centropyxis platystoma* | TA | CEPLAT | 6 | 3.0 | Penard 1890 |
| *Centropyxis sylvatica* | TA | CESY | 3 | 1.9 | Deflandre 1929; Bonnet and Thomas 1955 |
| *Conicocassis pontigulasiformis* | TA | COPO | 28 | 22.3 | Beyens, Chardez and De Bock 1986; Nasser and Anderson 2015 |
| *Corythion constricta* | WIST | COCO | 5 | 6.8 | Certes 1889; Jung 1942 |
| *Corythion dubium* | WIST | CODU | 37 | 47.5 | Taranek 1871 |
| *Cryptodifflugia ovilformis* | TA | CROV | 55 | 68.6 | Penard 1890 |
| *Cyclopyxis arcelloides* | TA | CYAR | 1 | 4.7 | Penard 1902; Deflandre 1929 |
| *Cyclopyxis eurostoma* | TA | CYEU | 20 | 8.9 | Deflandre 1929 |
| *Cyclopyxis kahli* | TA | CYKA | 1 | 1.3 | Deflandre 1929 |
| *Difflugia acuminata* | TA | DIAC | 18 | 3.8 | Ehrenberg 1838 |
| *Difflugia globulosa* | TA | DIGL | 26 | 29.0 | Dujardin 1837; Penard 1902 |
| *Difflugia lithophila* | TA | DILI | 66 | 32.7 | Penard 1902 |
| *Difflugia lucida* | TA | DILU | 70 | 34.5 | Penard 1890 |
| *Difflugia oblonga* | TA | DIOB | 52 | 11.2 | Ehrenberg 1838 |
| *Difflugia penardi* | TA | DIPE | 35 | 30.9 | Hopkinson 1909 |
| *Difflugia pristis* type | TA | DIPR | 29 | 9.3 | Penard 1902 |
| *Difflugia pulex* | TA | DIPU | 36 | 8.6 | Penard 1902 |
| *Difflugia pyriformis* | TA | DIPY | 7 | 5.9 | Perty 1849 |
| *Difflugia rubescens* | TA | DIRU | 12 | 8.4 | Penard 1891 |
| *Difflugia urceolata* | TA | DIUR | 9 | 6.2 | Carter 1864 |
| *Euglphya* degraded | WIST | EUDE | 15 | 5.8 | N/A |
| *Euglypha laevis* | WIST | EULA | 21 | 3.7 | Ehrenberg 1845 |
| *Euglypha rotunda* | WIST | EURO | 95 | 42.7 | Ehrenberg 1845; Wailes and Penard 1911 |
| *Euglypha strigosa* | WIST | EUST | 74 | 24.4 | Ehrenberg 1848 |
| *Euglypha tuberculata* | WIST | EUTU | 76 | 40.0 | Dujardin 1841 |
| *Gibbocarina galeata* | TA | GIGA | 21 | 11.8 | Penard 1890; Kosakyan et al. 2016 |
| *Gibbocarina gracilis* | TA | GIGR | 43 | 14.3 | Penard 1910 |
| *Heleopera petricola* | TA | HEPE | 31 | 4.8 | Leidy 1879 |
| *Heleopera rosea* | TA | HERO | 31 | 11.8 | Penard 1890 |
| *Heleopera sphagni* | TA | HESP | 1 | 0.6 | Leidy 1874 |
| *Heleopera sylvatica* | TA | HESY | 1 | 3.0 | Penard 1890 |
| *Hyalosphenia elegans* | TA | HYEL | 1 | 0.9 | Leidy 1874 |
| *Hyalosphenia ovalis* | TA | HYOV | 13 | 22.0 | Wailes 1912 |
| *Nebela collaris* | TA | NECO | 36 | 15.8 | Ehrenberg 1848; Kosakyan and Gomaa 2013 |
| *Nebela tincta* | TA | NETI | 48 | 73.6 | Leidy 1979; Awerintzew 1906; Kosakyan et al. 2012 |
| *Netzelia wailesi* | TA | NEWA | 5 | 8.4 | Ogden 1980; Meisterfeld 1984 |
| *Padaungiella lageniformis* | TA | PALA | 38 | 17.3 | Penard 1890 |
| *Paraquadrula irregularis* | TA | PAIR | 48 | 41.7 | Wallich 1863 |
| *Phryganella acropodia* type | TA | PHAC | 53 | 20.5 | Hertwig and Lesser 1874; Cash and Hopkinson 1909 |
| *Placocista spinosa* type | WIST | PLSP | 3 | 1.5 | Penard 1899 |
| *Planocarina marginata* | TA | PLMA | 1 | 2.9 | Penard 1902 |
| *Psuedodifflugia fulva* type | TA | PSFU | 3 | 0.9 | Archer 1870 |
| *Quadrulella symmetrica* | TA | QUSY | 1 | 0.8 | Wallich 1863; Schulze 1875; Kosakyan et al. 2016 |
| *Sphenoderia lenta* | WIST | SPLE | 1 | 0.8 | Schlumberger 1845 |
| *Tracheleuglypha denta* | WIST | TRDE | 7 | 11.1 | Vejdovsky 1882; Deflandre 1928 |
| *Trigonopyxis arcula* | TA | TRGA | 4 | 1.7 | Penard 1912 |
| *Trigonopyxis minuta* | TA | TRGM | 2 | 1.0 | Schönborn and Peschke 1988 |
| *Trinema complanatum* | WIST | TRCO | 5 | 2.4 | Penard 1890 |
| *Trinema enchelys* | WIST | TREN | 19 | 4.4 | Leidy 1878 |
| *Trinema lineare* | WIST | TRLI | 76 | 12.2 | Penard 1890 |
| *Valkanovia elegans* | TA | VAEL | 53 | 50.4 | Schönborn 1964 |
| *Wailesella eboracencis* | TA | WAEB | 17 | 21.0 | Wailes and Penard 1911 |

package Plum (Aquino-López et al., 2018). Plum assumes a constant rate of supply (CRS) of $^{210}$Pb within samples. However, unlike previous CRS models (Appleby, 2001; Appleby and Oldfield, 1978) Plum separates the age-depth modelling process from the $^{210}$Pb decay equation and implements a Bayesian modelling approach using a self-adjusting Markov Chain Monte Carlo (MCMC) algorithm. This Bayesian modelling approach allows for better quantification of uncertainty in modelled dates and more robust integration of $^{210}$Pb and $^{14}$C dates. See Aquino-López et al. (2018) for full details.

### 3.4. Testate amoebae

Testate amoebae were prepared for analysis following Booth et al. (2010) for surface vegetation and peat core samples – palaeo-samples were analysed every other centimetre down core; i.e. a 1-cm layer, every 2 cm. Approximately 5 $cm^3$ of each surface vegetation sample and around 2 $cm^3$ for each palaeo-sample was boiled in water for 10 min, passed through a 300 µm sieve and then back-sieved through a 15 µm mesh. These processed samples were then stored at 4 °C prior to examination under a high-powered, transmitted-light microscope at between 200 and 400 × magnification. A minimum of 100 individuals of taxa without weak idiosomic tests (WISTs) were counted per sample, with any WIST taxa recorded in addition. WISTs have been shown to preserve less favourably in peat as subfossils down core (Swindles et al., 2020) and within our study included: *Euglypha* spp., *Trinema* spp., *Corythion* spp., *Placocista spinosa* type, *Sphenodenria lenta* and *Trachleuglypha denta*. In order to examine the influence of excluding WISTs, we conducted multivariate statistical analysis and developed transfer functions for the entire dataset including WISTs and then separately excluding WISTs. Testate amoebae were identified where possible to species level, with reference to standard taxonomic materials (Charman et al., 2000; Siemensma, 2021).

### 3.5. Statistical analyses

Multivariate statistical analysis was undertaken in R version 3.6.3 (R Core Team, 2020) with the packages vegan (Oksanen et al., 2020) and analogue (Simpson and Oksanen, 2020) to explore the dataset and to examine the relationships between testate amoebae and environmental conditions. Taxa with a maximum abundance of less than 2% and fewer than five occurrences were excluded from multivariate analyses to reduce the influence of rare taxa (see Swindles et al., 2009). We performed ordination with Non-metric Multidimensional Scaling (NMDS) using the Bray-Curtis dissimilarity index. Additionally, Detrended Correspondence Analysis (DCA) showed that the data had a long axis length (DCA1 all taxa = 4.15; DCA1 WISTs removed = 4.71) suggesting heterogeneity in the data, high beta diversity and predominantly unimodal species distributions – consequently Canonical Correspondence Analysis (CCA) was then performed. CCA allowed us to partial out the amount of variance explained by specific environmental variables and to test the significance of each variable.

Transfer functions for WTD and pH were developed using the R package rioja (Juggins, 2020). The following common model types were applied: Weighted Averaging with tolerance downweighting (WA.tol) and without (WA), with the option for classical (cla) or inverse (inv) deshrinking, Weighted Averaging Partial Least Squares (WAPLS) and Maximum Likelihood (ML). These transfer function models were developed and cross-validated using the leave-one-out (LOO) method for the entire dataset and then with WIST taxa removed. The metrics $RMSEP_{LOO}$, $R^2_{LOO}$, average bias and maximum bias were used to evaluate transfer function performance. Model predictions generally had higher residual values towards the ends of the environmental gradients, especially for WTD. Therefore, in a second model run transfer functions were pruned of high residual values greater than 20% of the total range of measured WTD (>7.4 cm) and pH (>0.617). This cut-off point has been shown to strike a good balance between improving model performance and preserving the range of the environmental gradient for which a transfer function has predictive power (Amesbury et al., 2018, 2016, 2013; Booth, 2008; Charman et al., 2007; Payne et al., 2006; Swindles et al., 2015; Taylor et al., 2019a). Leave-one-site-out ($RMSEP_{LOSO}$) and segment-wise ($RMSEP_{SW}$) cross validation methods were applied to the pruned WTD and pH transfer function models with WISTs removed to further evaluate performance (Table 4; Supplementary Fig. 2). Spatial autocorrelation analysis was not performed due to the limited geographical range of our sampling region and the minimal effect this typically has on model performance (see Amesbury et al., 2018).

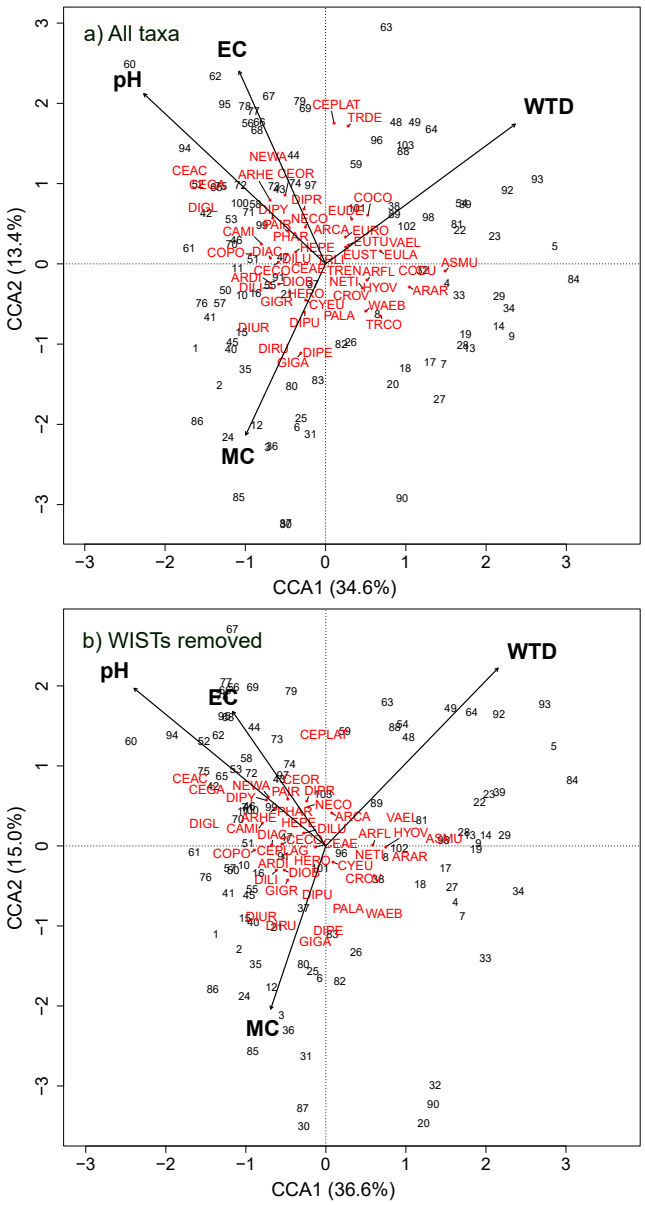


**Fig. 2.** CCA of species, samples and environmental variables for a) all taxa and b) with WISTs removed. Species with fewer than five occurrences and a maximum abundance < 2% were removed. See Table 2 for species codes.

Tolerance and optima statistics for WTD and pH were calculated for all taxa using WA.

The best performing transfer function models for WTD and pH were applied to a palaeo dataset of subfossil testate amoebae from the Colesdalen core. We compared our WTD reconstruction for the Colesdalen core with the outputs from other regional transfer function models: Subarctic Sweden (Swindles et al., 2015), pan-European (Amesbury et al., 2016), Arctic Alaska (Taylor et al., 2019a) and Subarctic Finland and West Russia (Zhang et al., 2017).

## 4. Results

### 4.1. Relationship between species distribution and environmental variables

A total of 60 testate amoeba taxa from 30 genera were identified in the surface vegetation samples from peatlands in Svalbard (Table 2), with a total count of 15,475 individuals. The species occurring in the

**Table 3**
Ordination statistics of environmental variables, both including and excluding taxa with weak idiosomic tests (WISTs).

| Environmental variables | pCCA | | | | NMDS | | | | | | | |
|---|---|---|---|---|---|---|---|---|---|---|---|---|
| | pCCA all taxa | | pCCA no WISTs | | NMDS all taxa | | | | NMDS no WISTs | | | |
| | Variance explained (%) | Significance | Variance explained (%) | Significance | NMDS1 | NMDS2 | $R^2$ | Significance | NMDS1 | NMDS2 | $R^2$ | Significance |
| EC | 15.96 | $p < 0.001$ | 16.96 | $p < 0.001$ | −0.24482 | 0.96957 | 0.3446 | $p < 0.001$ | −0.33694 | 0.94153 | 0.3213 | $p < 0.001$ |
| pH | 29.04 | $p < 0.001$ | 33.06 | $p < 0.001$ | −0.55835 | 0.82961 | 0.4102 | $p < 0.001$ | −0.69611 | 0.71794 | 0.3896 | $p < 0.001$ |
| MC | 6.67 | $p = 0.344$ | 5.92 | $p = 0.406$ | −0.34161 | −0.93984 | 0.3159 | $p < 0.001$ | −0.18209 | −0.98328 | 0.2918 | $p < 0.001$ |
| WTD | 24.99 | $p = 0.002$ | 26.44 | $p < 0.001$ | 0.60047 | 0.79965 | 0.5135 | $p < 0.001$ | 0.46814 | 0.88366 | 0.5445 | $p < 0.001$ |

most samples were *Centropyxis aerophila*, *Euglypha rotunda*, *Euglypha tuberculata*, *Trinema lineare*, *Euglypha strigosa*, *Difflugia lucida* and *Difflugia lithophila*. Other notable species occurring in fewer samples, but at a high maximum abundance were *Nebela tincta* (73.6%), *Cryptodifflugia oviformis* (68.6%), *Campascus minutus* (67%) and *Valkanovia elegans* (50.4%). CCA shows that pH, WTD and EC are the most important controls of testate amoeba distribution (Fig. 2; Table 3). Partial CCAs when run for all taxa show pH explained 29.04% of variance ($p < 0.001$), WTD explained 24.99% ($p = 0.002$), EC explained 15.96% ($p < 0.001$) and MC explained 6.67% ($p = 0.344$). When WISTs are removed the amount of variance explained by environmental variables increased slightly, with pH explaining 33.06% ($p < 0.001$), WTD explaining 26.44% ($p < 0.001$), EC explaining 16.96% ($p < 0.001$) and MC explaining 5.92% ($p = 0.406$). NMDS analysis supports these findings, with all environmental variables – including MC – shown to be important controls on species distribution, both when run for all taxa and then with WISTs removed ($p < 0.001$; Fig. 3; Table 3). NMDS suggests the most important environmental controls are WTD (all taxa $R^2 = 0.51$; WISTs removed $R^2 = 0.54$) and pH (all taxa $R^2 = 0.41$; WISTs removed $R^2 = 0.39$). Fig. 3 highlights the association of the Sassendalen sites – underlain by a limestone bedrock – with a higher pH and Colesdalen – underlain by sandstones, siltstones and shales – with a slightly lower pH (Table 1).

### 4.2. Transfer function development

Transfer functions were developed for both WTD ($TF_{WTD}$) and pH ($TF_{pH}$) as both variables were highly significant environmental controls on testate amoeba species distribution in the ordination analysis. $R^2_{LOO}$ and $RMSEP_{LOO}$ were used as the primary metrics to identify the best performing models. Models were run including all taxa ($TF_{ALL}$) and again with WISTs removed ($TF_{NO.WIST}$) and produced models of comparable performance (Supplementary Table 2). The $TF_{NO.WIST}$ iteration of the models for both $TF_{WTD}$ and $TF_{pH}$ was used because of concerns over the preservation of WISTs down core (Swindles et al., 2020), compounded by a complete absence of WISTs in our entire independent palaeo dataset of testate amoeba abundance analysed from Colesdalen core (see Fig. 9). For $TF_{WTD\text{-}NO.WIST}$ with high residual values removed (residuals > 7.4 cm), all models showed lower $RMSEP_{LOSO}$ and $RMSEP_{SW}$ when compared to $RMSEP_{LOO}$, with the exception of ML (Table 4). All WA based models performed worse in wet (WTD < 0 cm) segments, while WA.cla and WA.cla.tol also performed poorly in the driest segment (WTD > 20 cm) (Supplementary Fig. 2). The best performing model was component 2 of the WAPLS model ($R^2_{LOO} = 0.719$, $RMSEP_{LOO} = 3.20$ cm, $RMSEP_{LOSO} = 3.53$ cm, $RMSEP_{SW} = 3.39$ cm, average bias = 0.04 cm, maximum bias = 5.29 cm, $n = 85$; Table 4; Fig. 6). ML models for $TF_{WTD\text{-}NO.WIST}$ demonstrated slightly higher $R^2_{LOO}$ values. However, the ML model had a greater number of high residual values (>7.4 cm) in initial model runs and demonstrated slightly higher $RMSEP_{LOO}$ values (Table 4) – therefore the WAPLS model was preferred. $TF_{WTD\text{-}NO.WIST}$ performs well, but with a slight over prediction of low WTD values and slight under prediction of high WTD values. For the $TF_{WTD\text{-}NO.WIST}$ model three species with low maximum abundances (*Heleopera sylvatica* = 3%, *Hyalosphenia elegans* = 0.9% and *Psuedodifflugia fulva* type = 0.9%) were removed owing to high residual values. Clear dry indicator species include *Assulina muscorum*, *Corythion dubium* (WIST taxon), *Valkanovia elegans*, *Hyalosphenia ovalis* and *Archerella flavum*, while important wet indicator species include *Difflugia rubescens*,

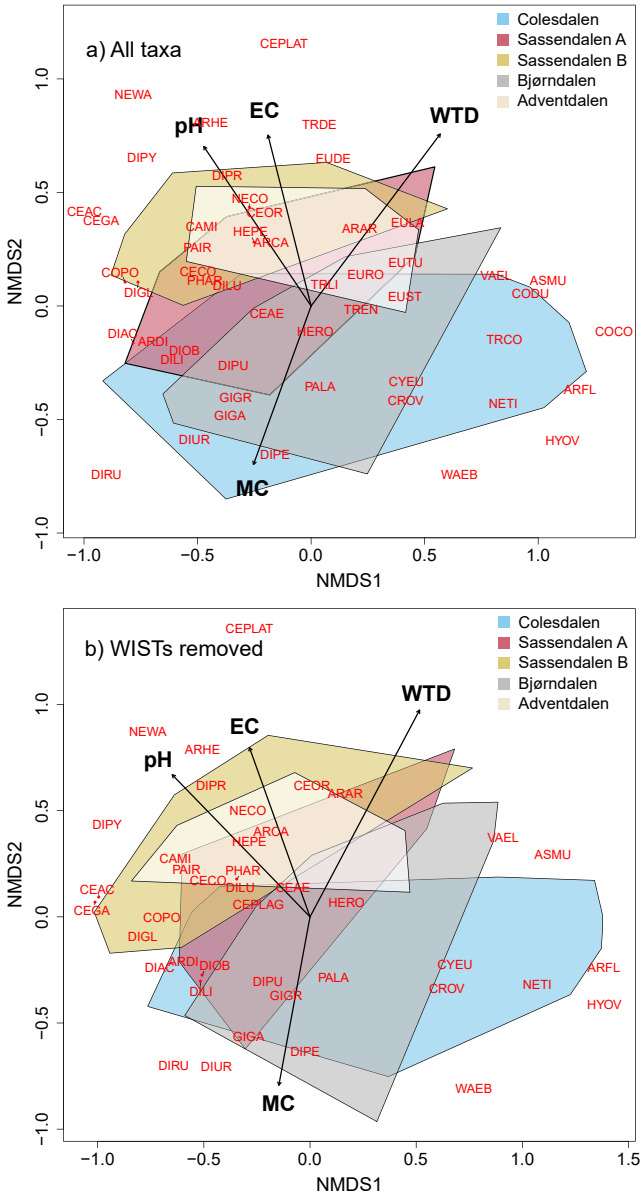


**Fig. 3.** NMDS of species, samples and environmental variables for a) all taxa and b) with WISTs removed. Species with fewer than five occurrences and a maximum abundance < 2% removed. See Table 2 for species codes.

**Table 4**
Transfer function performance metrics for pruned WTD and pH models with WIST taxa removed. Root mean squared error of prediction (RMSEP) statistics are based on leave-one-out ($RMSEP_{LOO}$), leave-one-site-out ($RMSEP_{LOSO}$) and segment-wise ($RMSEP_{SW}$) cross validation methods. Changes in model performance from $RMSEP_{LOO}$ to both $RMSEP_{LOSO}$ and $RMSEP_{SW}$ are given in parentheses.

| | $TF_{WTD\text{-}NO.WIST}$ | | | | | | |
|---|---|---|---|---|---|---|---|
| Model | $RMSEP_{LOO}$ | $RMSEP_{LOSO}$ | $RMSEP_{SW}$ | $R^2_{LOO}$ | Avg. Bias | Max. Bias | *n* |
| *WA.inv* | 3.697 | 4.617 (0.920) | 4.027 (0.330) | 0.634 | 0.001 | 6.028 | 88 |
| *WA.cla* | 4.303 | 4.740 (0.437) | 4.782 (0.479) | 0.652 | 0.074 | 8.633 | 67 |
| *WA.inv.tol* | 3.565 | 4.495 (0.930) | 3.860 (0.295) | 0.669 | 0.073 | 5.774 | 88 |
| *WA.cla.tol* | 4.299 | 5.110 (0.811) | 4.596 (0.297) | 0.653 | 0.217 | 9.551 | 70 |
| *WAPLS.C2* | 3.198 | 3.526 (0.328) | 3.392 (0.194) | 0.719 | 0.036 | 5.293 | 85 |
| *ML* | 3.776 | 3.669 (-0.107) | 3.740 (-0.036) | 0.721 | 0.276 | 3.05 | 74 |
| | $TF_{pH\text{-}NO.WIST}$ | | | | | | |
| Model | $RMSEP_{LOO}$ | $RMSEP_{LOSO}$ | $RMSEP_{SW}$ | $R^2_{LOO}$ | Avg. Bias | Max. Bias | *n* |
| *WA.inv* | 0.278 | 0.408 (0.131) | 0.340 (0.062) | 0.541 | −0.002 | 0.553 | 85 |
| *WA.cla* | 0.271 | 0.347 (0.075) | 0.279 (0.007) | 0.771 | 0.002 | 0.343 | 61 |
| *WA.inv.tol* | 0.271 | 0.448 (0.177) | 0.340 (0.069) | 0.577 | 0.007 | 0.539 | 86 |
| *WA.cla.tol* | 0.32 | 0.439 (0.119) | 0.331 (0.011) | 0.69 | 0.018 | 0.316 | 70 |
| *WAPLS.C2* | 0.284 | 0.392 (0.107) | 0.333 (0.049) | 0.595 | 0 | 0.412 | 88 |
| *ML* | 0.3 | 0.521 (0.221) | 0.357 (0.058) | 0.619 | −0.036 | 0.401 | 80 |

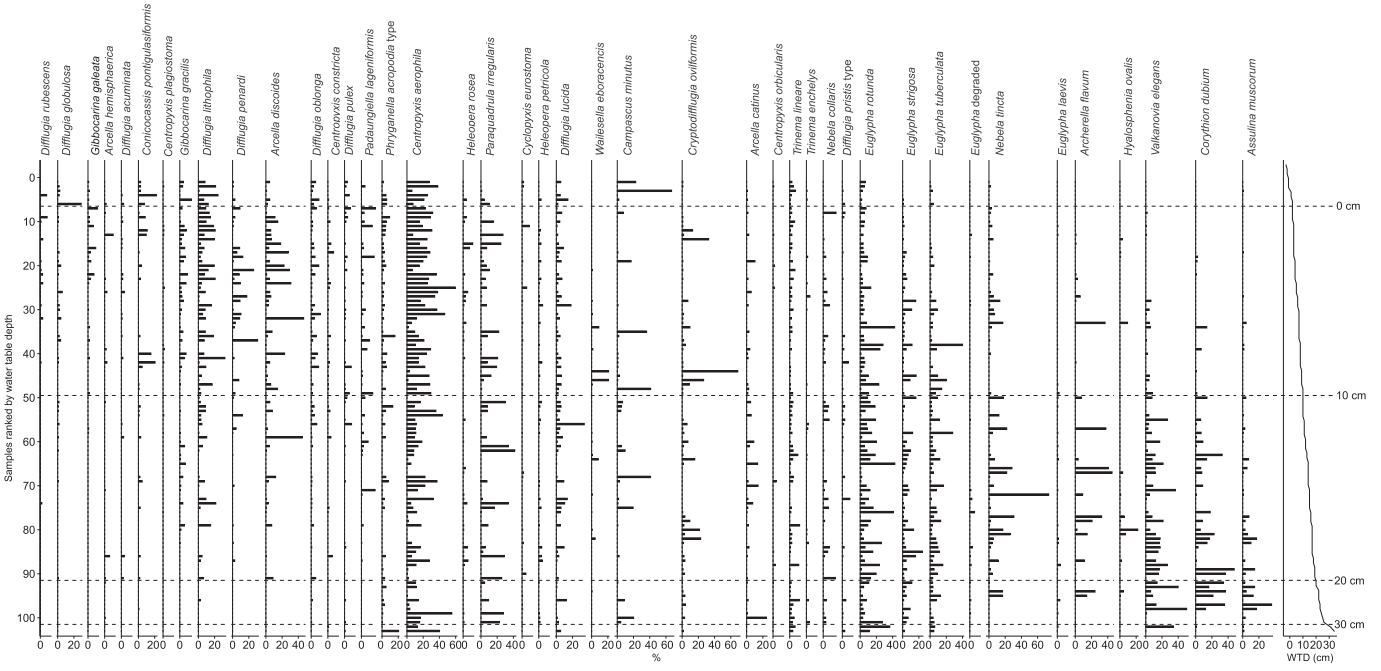


**Fig. 4.** Abundance of selected testate amoeba taxa (at least 10 occurrences) ranked by observed water-table depth (WTD) indicating a range of WTD conditions. Dotted lines denote 10 cm intervals in measured WTD.

*Difflugia globulosa*, *Gibbocarina galeata*, *Arcella hemisphaerica* and *Difflugia acuminata* (Fig. 4). WTD optima and tolerance statistics for individual species are presented in Fig. 7.

For $TF_{pH\text{-}NO.WIST}$ with high residual values removed (>0.617), all models showed lower $RMSEP_{LOO}$ when compared to $RMSEP_{LOSO}$ and $RMSEP_{SW}$ (Table 4). The WA.inv, WA.inv.tol, WAPLS and ML models performed slightly worse in lowest pH segment (i.e. 5–5.49), yet the WA.cla and WA.cla.tol models were more consistent across a range of pH values (Supplementary Fig. 2). The preferred model was WA with classical deshrinking and tolerance downweighting (WA.cla.tol) ($R^2_{LOO}$ = 0.690, $RMSEP_{LOO}$ = 0.320, $RMSEP_{LOSO}$ = 0.439, $RMSEP_{SW}$ = 0.331, average bias = 0.018, maximum bias = 0.316, *n* = 70; Table 4; Fig. 6). WA with classical deshrinking (WA.cla) demonstrated a higher $R^2_{LOO}$ (0.771); however, WA.cla.tol required the removal of fewer high residual (>0.617) values and was therefore preferred. For the $TF_{pH\text{-}NO.WIST}$ model two species with low maximum abundances (*Heleopera sylvatica* = 3% and *Quadrulella symmetrica* = 0.8%) were also removed due to high residual values. Peatland pH is generally linked with trophic status (Gorham et al., 1987; Lamentowicz et al., 2013) and is something considered further in the discussion section. High pH (more minerotrophic) indicator species include *Campascus minutus*, *Arcella catinus* and *Paraquadrula irregularis*, while lower pH (less minerotrophic) indicator species include *Wailesella eboracencis*, *Assulina muscorum* and *Hyalosphenia ovalis* (Fig. 5). For pH some species demonstrate bimodal peaks in abundance at low and high pH levels; e.g., *Assulina muscorum* and *Corythion dubium* (Fig. 5).

### 4.3. Transfer function application

The $TF_{WTD\text{-}NO.WIST}$ and $TF_{pH\text{-}NO.WIST}$ models (Fig. 6) were applied to a peat core sampled in Colesdalen to reconstruct past WTD and pH from ~ 800 CE to present (Fig. 9). The most common subfossil taxa present in

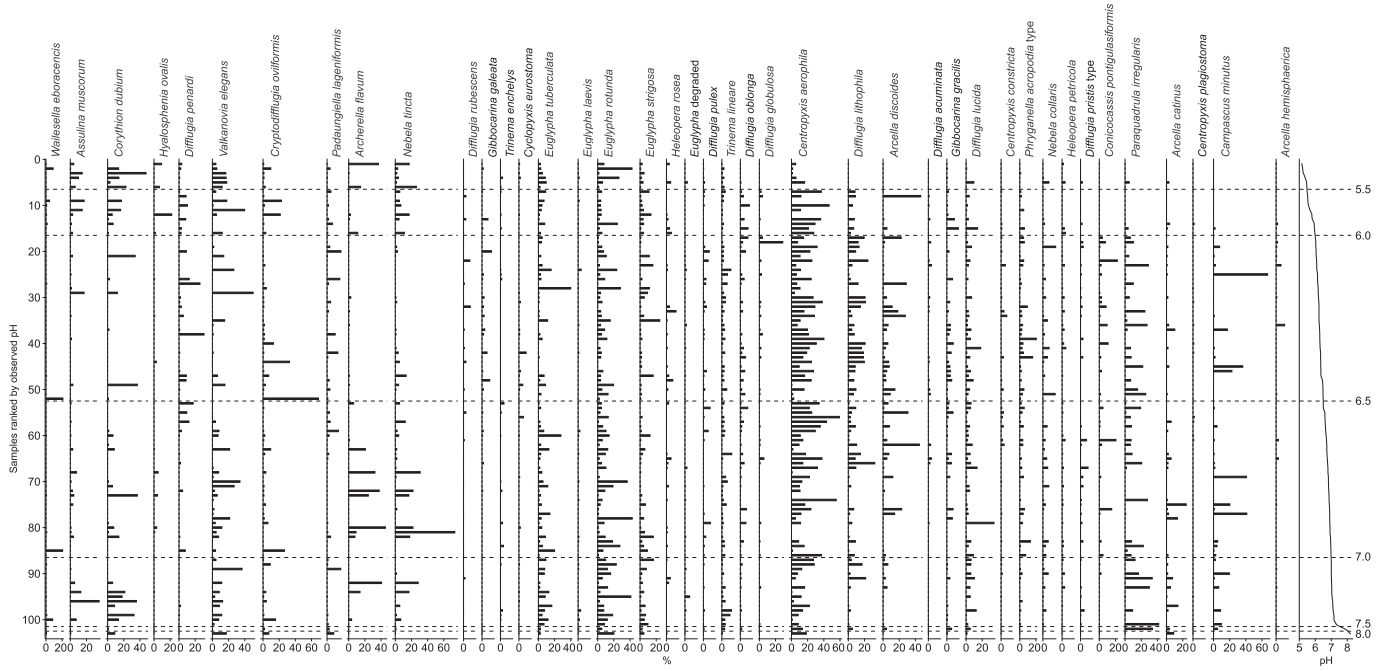


**Fig. 5.** Abundance of selected testate amoeba taxa (at least 10 occurrences) ranked by observed pH indicating a range of pH conditions. Dotted lines denote 0.5 intervals in measured pH.

the core include *Gibbocarina galeata*, *Gibbocarina gracilis*, *Conicocassis pontigulaformis*, *Nebela tincta* and *Centropyxis aerophila*. Notably, there was a complete absence of WISTs in the palaeo record. Both $TF_{WTD\text{-}NO.WIST}$ and $TF_{pH\text{-}NO.WIST}$ transfer functions were applied with no missing analogues. The quality of analogues was tested by comparing maximum relative abundances of species in the palaeo and calibration datasets (Supplementary Fig. 3). The majority of taxa demonstrate well constrained species optima (Hill's N2 > 5), including all taxa (with the exception of *Alablasta militaris*) showing a higher maximum abundance in the palaeo dataset than the calibration dataset.

The $TF_{WTD\text{-}NO.WIST}$ reconstruction shows a relatively stable WTD from the base of the core at ~800 CE to ~1500 CE cm, where there is a period of drying, followed by another dry period at ~1750 CE (Fig. 9). This spike in WTD ~1750 CE is associated with increased abundance of *Nebela tincta* and a decrease in *Gibbocarina galeata*. From ~1750 CE onwards there is a general wetting trend, particularly from ~1920 CE. The $TF_{pH\text{-}NO.WIST}$ reconstruction shows a shift to lower pH conditions ~1400 CE, with the lowest pH value coinciding with the dry phase ~1750 CE. From ~1750 CE to present, pH fluctuates but demonstrates a general trend of an increasing pH with a slight lowering of pH from ~2000 CE onwards. There is a significant inverse relationship between WTD and pH ($p < 0.01$), with dry conditions associated with a lower pH and vice versa. Axis 1 scores from a DCA and NMDS analysis of the fossil data from the Colesdalen core correlate significantly with both WTD (DCA $p < 0.001$; NMDS $p < 0.001$) and pH (DCA $p < 0.001$; NMDS $p < 0.001$), suggesting both our reconstructions are good representations of changes in the structure of the fossil data (Supplementary Fig. 4).

We compared the $TF_{WTD\text{-}NO.WIST}$ reconstruction of the Colesdalen core with transfer functions originally developed for other regions (Fig. 10). There were a number of missing analogues for the Colesdalen core in the Subarctic Sweden ($n = 12$), pan-European ($n = 3$), Arctic Alaska ($n = 9$) and Subarctic Finland and West Russia ($n = 10$) calibration datasets (See Supplementary Table 3). The range in reconstructed WTD values is greater in transfer functions from other regions, in particular for Arctic Alaska (Fig. 10a), yet reconstructed z-scores for the Svalbard transfer function are very similar to those from other regions (Fig. 10b). In fact, WTD z-scores produced by $TF_{WTD\text{-}NO.WIST}$ correlate significantly with z-scores produced by the Subarctic Sweden ($p = 0.002$), pan-European ($p < 0.001$), Arctic Alaska ($p < 0.001$) and Subarctic Finland and West Russia ($p < 0.001$) models.

## 5. Discussion

We developed the first testate amoeba transfer functions for peatlands in Svalbard, the northernmost study of its kind to date. Despite lower testate amoeba diversity being observed in the High Arctic (Beyens and Bobrov, 2016), we identified 60 testate amoeba taxa in surface vegetation samples (Table 2) – including the regionalised High Arctic taxa of *Centropyxis gasperella* and *Conicocassis pontigulaformis*. In the palaeo core from Colesdalen spanning the period ~ 800 CE to present, 27 taxa were identified and species diversity was relatively stable down core (Fig. 9). Furthermore, testate amoeba were abundant enough for the minimum count of 100 individuals in all palaeo samples. This diversity and abundance in both contemporary and palaeo samples is uncharacteristic of other High Arctic regions (e.g. Sim et al., 2019) and may be as a result of the unusual climate of Svalbard for its latitude, which is moderated by the West Spitsbergen Current (Walczowski and Piechura, 2011).

### 5.1. Testate amoebae and water-table depth

We found that peatland WTD was a key control on testate amoeba species distribution in Svalbard (Figs. 2 and 3; Table 3) and developed a palaeohydrological transfer function. The majority of taxa occupy WTD niches as expected from lower latitude peatlands (e.g. Amesbury et al., 2018, 2016; Charman et al., 2007; Qin et al., 2021) and other permafrost peatlands (e.g. Lamarre et al., 2013; Swindles et al., 2015a; Taylor et al., 2019a; Zhang et al., 2017). Nonetheless, we were able to better quantify the hydrological niches of High Arctic testate amoeba in Svalbard, building on initial pioneering studies from the twentieth century. We corroborate previous suggestions that *Assulina muscorum* prefers drier habitats in Svalbard (Beyens et al., 1986c) and that *Arcella hemisphaerica* is a predominantly wet taxon (Schönborn, 1966). Similarly, our data confirm previous observations from Svalbard suggesting *Centropyxis aerophila* occurs across both wet and dry habitats (Beyens et al., 1986c, 1986b). The predominantly Arctic taxa *Conicocassis pontigulaformis* and

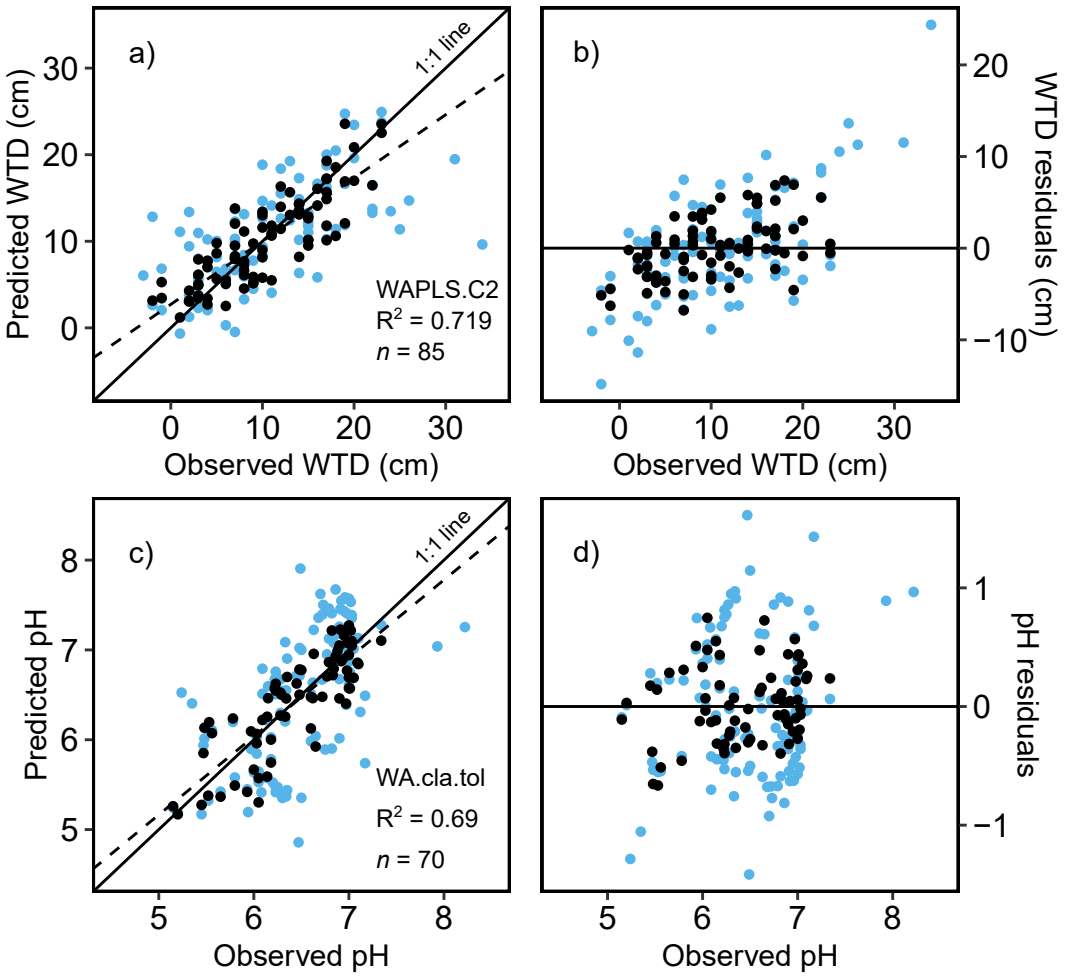


**Fig. 6.** Transfer function performance. a) Observed and predicted water-table depth (WTD) for each site using the WAPLS.C2 model (WIST taxa removed) and b) residuals for each site against observed WTD. c) Observed and predicted pH for each site using the WA.cla.tol model (WIST taxa removed) and d) residuals for each site against observed pH. Blue-coloured points are model runs with all data and black-coloured points are model runs after the removal of samples with high residual values. Dotted lines represent the linear trends of the data points and solid lines represent 1:1 lines.

*Centropyxis gasparella* (Beyens and Bobrov, 2016; Bobrov and Wetterich, 2012) were observed in our surface samples, both with a wet WTD optimum of ~ 5 cm (Fig. 7). This WTD optimum for *C. pontigulaformis* in Svalbard agrees with transfer function data from Arctic Alaska (Taylor et al., 2019a). Similarly, *C. gasparella* has been observed in standing water and wet mosses (Beyens et al., 1986b; Chardez and Beyens, 1988), but we present the first inclusion of this species in a transfer function.

### 5.2. Testate amoebae and trophic status (pH)

We found that pore water pH was an important control on testate amoeba species distribution (Figs. 2 and 3; Table 3) and developed a transfer function to reconstruct past pH. Peatland pH has a strong relationship with trophic status; oligotrophic bogs are acidic, while minerotrophic poor fens and rich fens demonstrate an increasing alkalinity and concentration of dissolved minerals (see Gorham et al., 1987; Lamentowicz et al., 2013). In contrast to lower-latitudes, there are few true low pH bogs in the High Arctic (Woo and Young, 2006) and in Svalbard. Our contemporary sampling data showed a strong oligotrophic to minerotrophic gradient both within and between sampling sites, from poor fen to extremely rich fen conditions (Table 1). Poor fens are generally dominated by *Sphagnum* mosses and shrubs; moderately rich fens are characterised by brown mosses (e.g. *Drepanocladus* sp.) and sedges; while extremely rich fens also exhibit brown mosses (e.g. *Scorpidium* sp.) and sedges (Warner and Rubec, 1997). However, nutrient levels and pH will not always be coincident along a fen-bog gradient (Bridgham et al., 1996). For example, phosphorus (P) concentrations are typically higher in fens than bogs, but rapid microbial mineralisation can result in similar levels of available P (Kellogg and Bridgham, 2003). Nonetheless, pH is a key control on bryophyte vegetation (Vitt and Chee, 1990) and an important characteristic used in the classification of wetland type (e.g. Tiner, 2016) – therefore, we suggest it is appropriate to use pH as a proxy for trophic status in the context of changing permafrost dynamics and shifting hydrological patterns.

The response of individual testate amoeba species to changing trophic conditions is predominantly in line with previous studies. Similarly to Taylor et al. (2019a), we found that *Gibbocarina galeata* and *Archerella flavum* were indicative of more oligotrophic conditions (Fig. 8). We found that *Assulina muscorum* is abundant in more oligotrophic conditions supporting earlier work by Beyens et al. (1986c) and Mitchell (2004), but the taxon was also present in minerotrophic conditions (Fig. 5) as was observed by Taylor et al. (2019a). *A. muscorum* has a clearly defined unimodal WTD optima and only appeared with more than 5% abundance in samples with a WTD over 13 cm (Fig. 4),

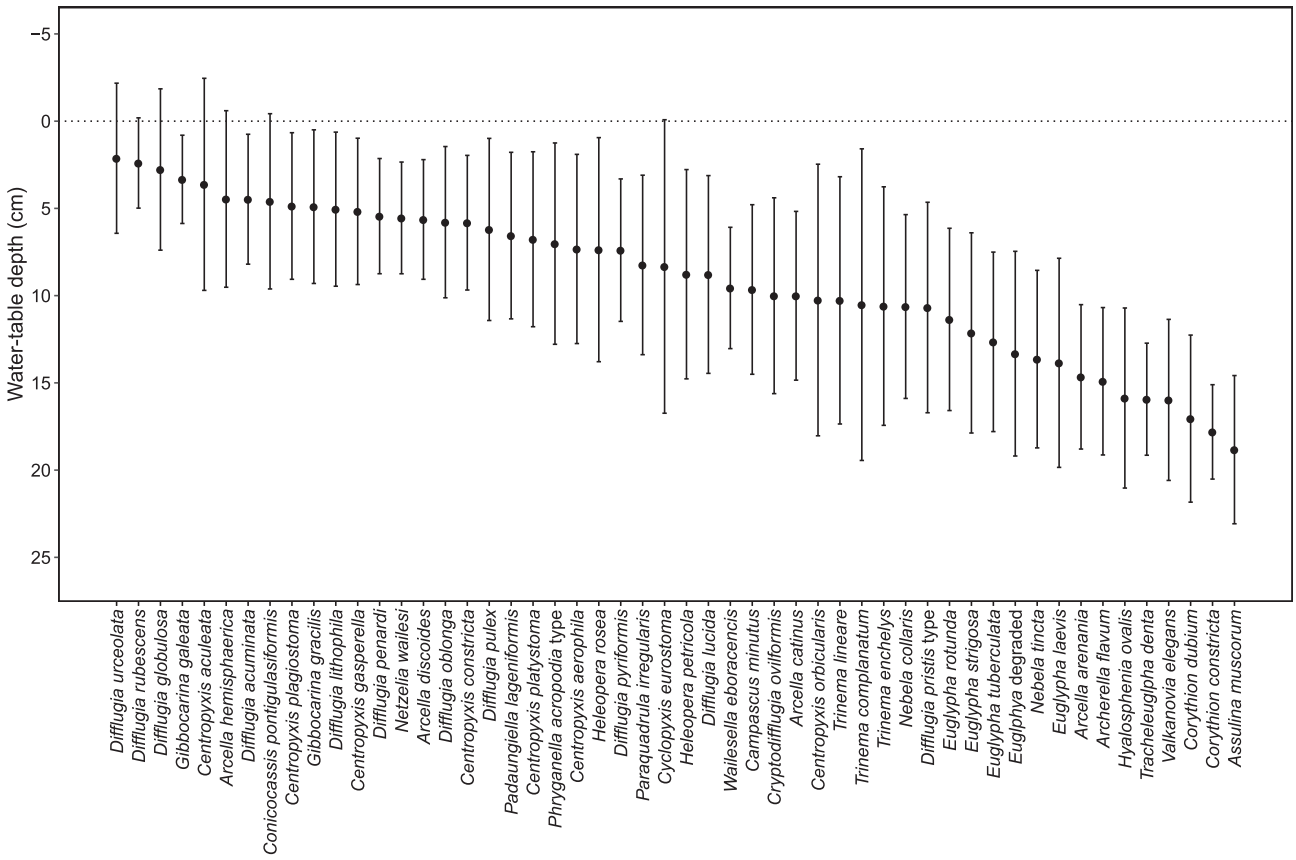


**Fig. 7.** Water-table depth (WTD) optima and tolerance calculated through weighted averaging for taxa at least five occurrences.

therefore suggesting hydrological conditions were the primary control on the distribution of this taxon. *Paraquadula irregularis* was more abundant in the more minerotrophic samples (Figs. 5 and 8), corroborating previous observations from Svalbard (Beyens et al., 1986b). Nonetheless, *P. irregularis* occurred across a broad range of WTDs (Fig. 4), suggesting species distribution is primarily driven by pH. It has been suggested that modification of surface soils by sea birds in Svalbard, linked partly to nutrient addition, may reduce the abundance of *Phyragrenella acropodia* and *Centropyxis aerophila* (Mazei et al., 2018). Nutrient levels were not directly measured in our study, but no clear abnormalities in abundance were observed. Both *P. acropodia* type ($n$ = 53, max abundance = 20.5%) and *C. aerophila* ($n$ = 95, max abundance = 59.3%) were common taxa in the surface samples (Table 2) and present across a broad range of both WTD and pH values (Figs. 4 and 5).

### 5.3. Application of transfer functions

The pan-Europe (Amesbury et al., 2016), Subarctic Sweden (Swindles et al., 2015), Arctic Alaska (Taylor et al., 2019a) and Subarctic Finland and West Russia (Zhang et al., 2017) transfer functions were also applied to Colesdalen core and produced WTD reconstructions of higher magnitude shifts than the $TF_{WTD\text{-}NO.WIST}$ model (Fig. 10a). The higher magnitude reconstructed WTD shifts in transfer functions from other regions was likely a result of a wider range of sampled WTD than those experienced in Svalbard, effectively stretching the gradient. When z-scores were standardised for each regional transfer function they all produced comparable reconstructions that correlated significantly with our reconstruction (Fig. 10b). Nonetheless, there were a number of missing modern analogues for the palaeo dataset in the transfer functions from other regions that were relatively abundant in peatlands in Svalbard (Supplementary Table 3). Notably, *C. pontigulaformis* is absent from the Subarctic Sweden, pan-European and Subarctic Finland and West Russia transfer functions, while *Centropyxis plagiostoma* is absent across all other regional transfer functions. These are both relatively wet taxa (optima ~ 5 cm) and therefore when present in greater abundance in the fossil record, transfer functions experiencing missing analogues showed noticeable discrepancies in standardised values to our reconstruction, e.g. ~1200 CE (67 cm; Fig. 10b). However, *C. plagiostoma* was not abundant in our calibration dataset ($n$ = 11, max = 1.6%) and optima for both WTD and pH would likely be better defined with further sampling. Nonetheless, we suggest that WTD transfer function models from other regions are less applicable to peatlands in Svalbard, highlighting the importance of developing regional transfer functions – particularly in relatively unexplored environments.

The absence of taxa with weak idiosomic tests (WISTs) down core (Fig. 9) and prevalence of degraded *Euglypha* spp. in surface samples (Table 1) evidences the poor preservation of these tests and echoes previous taphonomic concerns over the long-term preservations of WISTs in older peats (Payne, 2007; Swindles et al., 2020; Swindles and Roe, 2007). Removing WISTs had minimal impact on transfer function performance statistics (Supplementary Table 2) and actually slightly improved the degree of variance in species abundance explained by WTD and pH (Fig. 2; Table 3). Therefore, we chose to use transfer functions excluding WISTs and can have confidence that the removal of WISTs retains the effectiveness of our transfer function models, while avoiding potential taphonomic issues. Testate amoebae diversity (Shannon Index) remains relatively consistent down the core (Fig. 9), evidencing good preservation of non-WIST taxa. There is a drop in testate amoeba diversity ~1750 CE (33 cm), corresponding to a dominance of *Nebela tincta* (Fig. 9). Yet, this period of reduced diversity does not correspond to any shift in peat physical of chemical properties (e.g. bulk density, C, N, LOI) that might indicate increased decomposition – suggesting genuine changes in WTD and pH are driving the shift in testate amoeba populations.

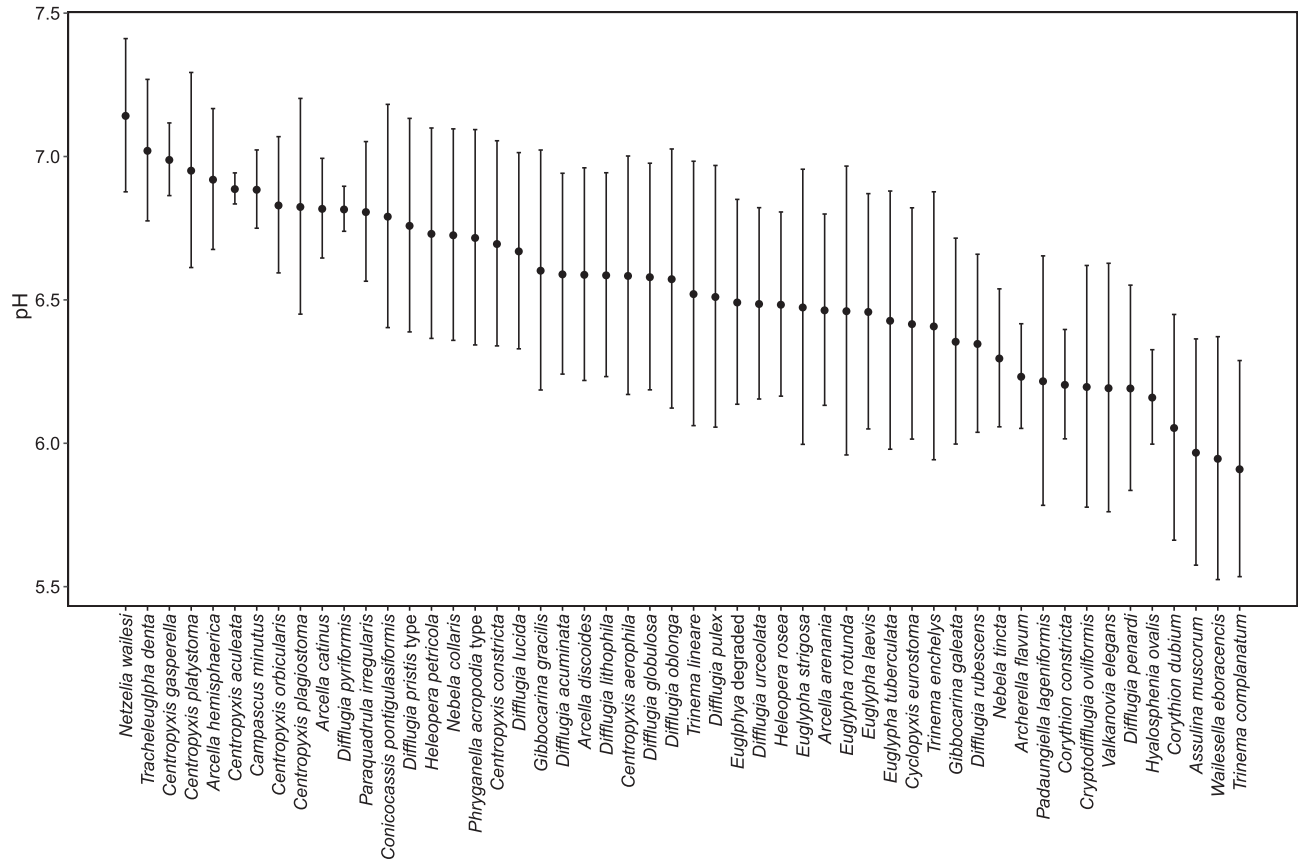


**Fig. 8.** pH optima and tolerance calculated through weighted averaging for taxa at least five occurrences.

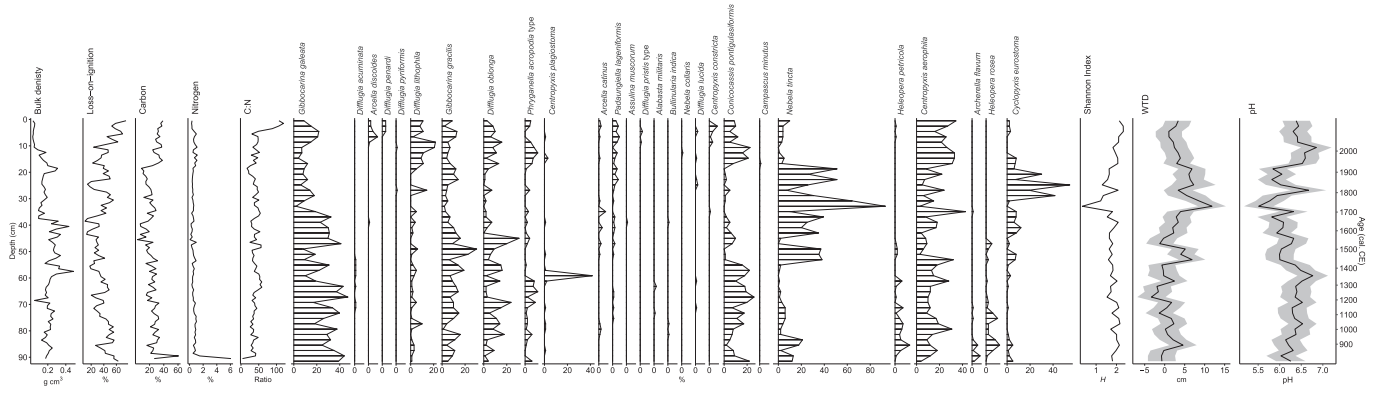


**Fig. 9.** Stratigraphic diagram of testate amoeba abundance in the Colesdalen core and best reconstructions for WTD and pH. Taxa ordered left (wetter) to right (drier) by WTD optima. Error based on 999 bootstrap cycles.

Peatland pH is strongly linked with trophic status (Gorham et al., 1987; Lamentowicz et al., 2013), therefore $TF_{pH\text{-}NO.WIST}$ is likely to be an effective proxy for interpreting past trophic conditions, particularly when paired with plant macrofossil analysis (see Väliranta et al., 2017). Payne (2011) raised concerns over the application of palaeohydrological transfer functions through periods of fen-bog transition in Mediterranean peatlands. However, in High Arctic Svalbard there is a narrower trophic gradient from poor to rich fen systems (Table 1) and WTD remains a significant control on species distribution across the entire pH range (Figs. 2 and 3; Table 3), therefore WTD reconstructions in Svalbard are likely to be more robust. Furthermore, $RMSEP_{SW}$ analysis suggests $TF_{pH\text{-}NO.WIST}$ (WA.cla.tol) performs consistently across a range of pH values (Supplementary Fig. 2). Thus, application of $TF_{pH\text{-}NO.WIST}$ and $TF_{WTD\text{-}NO.WIST}$ enables the reconstruction of peatland dynamics during the Holocene, including indications of changing trophic status – echoing similar findings from peatlands in Arctic Alaska (Taylor et al., 2019b).

The significant inverse correlation between reconstructed WTD and pH for the Colesdalen core ($p < 0.01$; Fig. 9) raises interesting questions over ecosystem and catchment dynamics. Specifically, recent wetting from ~1920 CE in the Colesdalen core corresponds to a shift to more minerotrophic conditions. Increases in precipitation across Svalbard in the twentieth century (Førland et al., 2011) may partially explain recent wetting. Similarly, the reorganisation of drainage systems caused by glacial retreat is associated with increased chemical weathering and higher meltwater pH in Svalbard (Nowak and Hodson, 2014). The

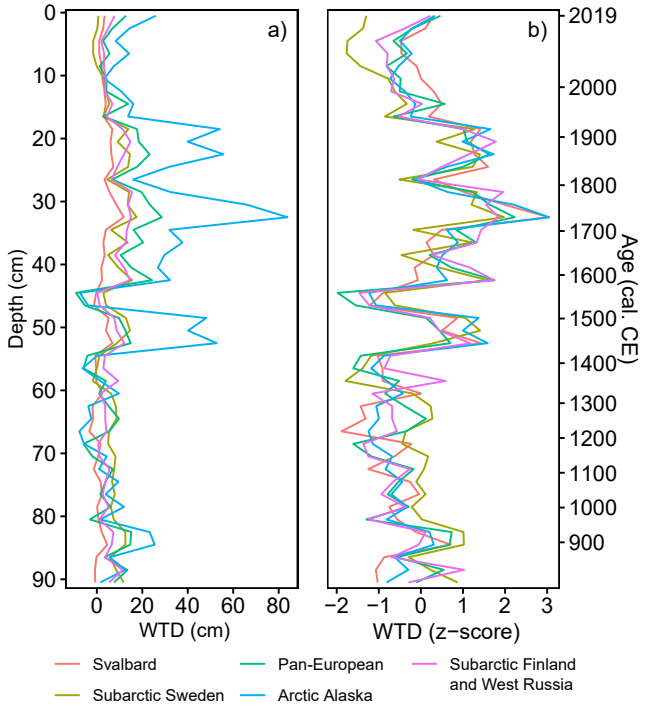


**Fig. 10.** Comparison of WTD reconstructions for the Colesdalen core from different regional transfer functions: Svalbard (this study), Subarctic Sweden (Swindles et al., 2015), pan-European (Amesbury et al., 2016), Arctic Alaska (Taylor et al., 2019a) and Subarctic Finland and West Russia (Zhang et al., 2017). a) WTD reconstructions in cm, b) WTD reconstruction z-scores. Note – the year of sampling (2019) has been added to Age (cal. CE) y-axis to highlight the non-linearity of age-depth relationship.

Colesdalen core is located towards the edge of a U-shaped valley (Fig. 1) and can be expected to receive both surface and groundwater flow from the surrounding catchment. Sandstones of the Central Tertiary Basin underlying Colesdalen are rich in feldspar and have a carbonate cement (Schlegel et al., 2013). Consequently, greater chemical weathering in the Colesdalen catchment as a result of changing drainage patterns linked to ice retreat, and increases in precipitation, offer potential explanations for recent increases in peatland wetness and pH.

### 5.4. Future research

The development of these transfer functions for WTD and pH opens up the possibility for comprehensive multiproxy palaeoecological reconstructions in Svalbard. Moreover, application of these transfer function models will be useful in examining the response of Svalbard's peatlands to rapid climate change during the twentieth century. Other avenues for future research could work to better quantify the influence of birds on soil nutrients and testate amoeba species in Svalbard (see Mazei et al., 2018), investigate the influence of increased salinity from salt spray or storm inundation on testate amoebae diversity and richness (see Swindles et al., 2018) and look to add regional transfer function data from higher-latitude peatlands to an updated pan-European transfer function model (Amesbury et al., 2016). Improved ecohydrological understanding of these ecosystems in recent decades, centuries and millennia will enable more thorough testing of hypotheses relating to increased productivity and expansion of high-latitude peatlands with warming (e.g. Gallego-Sala et al., 2018). Therefore, a study across multiple sites focusing on peatland ecohydrological and carbon dynamics in Svalbard during the Holocene would be particularly valuable.

## 6. Conclusions

1. We present the first testate amoebae transfer functions for reconstructing WTD and pH in peatlands in Svalbard, the northernmost study of its kind to date.
2. The majority of testate amoebae occupy WTD niches as expected from lower-latitude studies, although we were able to better quantify the hydrological niches of regionalised High Arctic taxa, e.g. *Centropyxis gasperella* and *Conicocassis pontigulaformis*.
3. Pore water pH was a significant control on testate amoeba species distribution and a proxy for trophic status – therefore our transfer function can be used to reliably reconstruct changes in past peatland pH in the context of changing permafrost dynamics and shifting hydrological patterns.
4. WISTs appear to preserve poorly in these peatlands, yet removal of WISTs from our transfer function models had minimal impact upon their performance. Therefore, we were able to confidently remove WISTs from our models to avoid potential taphonomic problems and recommend excluding them from minimum sample counts.
5. These transfer functions are valuable tools for multiproxy reconstructions investigating the response of peatlands in Svalbard to Holocene climate change and have the potential to improve understanding of long-term ecohydrological dynamics in these rapidly changing carbon-rich ecosystems.

## CRediT authorship contribution statement

**Thomas G. Sim:** Conceptualization, Methodology, Formal analysis, Investigation, Writing - original draft, Visualization. **Graeme T. Swindles:** Conceptualization, Methodology, Investigation, Writing - review & editing, Supervision. **Paul J. Morris:** Conceptualization, Writing - review & editing, Supervision. **Andy J. Baird:** Conceptualization, Writing - review & editing, Supervision. **Dan J. Charman:** Investigation, Writing - review & editing. **Matthew J. Amesbury:** Methodology, Investigation, Writing - review & editing. **Dave Beilman:** Investigation, Writing - review & editing. **Alex Channon:** Formal analysis. **Angela V. Gallego-Sala:** Investigation, Writing - review & editing, Resources.

## Declaration of Competing Interest

The authors declare that they have no known competing financial interests or personal relationships that could have appeared to influence the work reported in this paper.

## Acknowledgments

T.G.S. is in receipt of a UK Natural Environment Research Council Training Grant, NE/L002574/1. A.G.S., D.C. and A.C. acknowledge funding support from a UK Natural Environment Research Council Grant, NE/S001166/1 (ICAAP: Increasing Carbon Accumulation in Arctic Peatlands). We thank Macro Aquino-López and Maarten Blaauw for useful discussions regarding age-depth modelling. We also thank Xavier Comas for valuable assistance with fieldwork.

## Appendix A. Supplementary data

Supplementary data to this article can be found online at https://doi.org/10.1016/j.ecolind.2021.108122.

## References

Amesbury, M.J., Booth, R.K., Roland, T.P., Bunbury, J., Clifford, M.J., Charman, D.J., Elliot, S., Finkelstein, S., Garneau, M., Hughes, P.D.M., Lamarre, A., Loisel, J., Mackay, H., Magnan, G., Markel, E.R., Mitchell, E.A.D., Payne, R.J., Pelletier, N., Roe, H., Sullivan, M.E., Swindles, G.T., Talbot, J., van Bellen, S., Warner, B.G., 2018. Towards a Holarctic synthesis of peatland testate amoeba ecology: development of a new continental-scale palaeohydrological transfer function for North America and

comparison to European data. Quat. Sci. Rev. 201, 483–500. https://doi.org/10.1016/j.quascirev.2018.10.034.
Amesbury, M.J., Mallon, G., Charman, D.J., Hughes, P.D.M., Booth, R.K., Daley, T.J., Garneau, M., 2013. Statistical testing of a new testate amoeba-based transfer function for water-table depth reconstruction on ombrotrophic peatlands in north-eastern Canada and Maine, United States. J. Quat. Sci. 28, 27–39. https://doi.org/10.1002/jqs.2584.
Amesbury, M.J., Swindles, G.T., Bobrov, A., Charman, D.J., Holden, J., Lamentowicz, M., Mallon, G., Mazei, Y., Mitchell, E.A.D., Payne, R.J., Roland, T.P., Turner, T.E., Warner, B.G., 2016. Development of a new pan-European testate amoeba transfer function for reconstructing peatland palaeohydrology. Quat. Sci. Rev. 152, 132–151. https://doi.org/10.1016/J.QUASCIREV.2016.09.024.
Appleby, P.G., 2001. Chronostratigraphic techniques in recent sediments. In: Last, W.M., Smol, J.P. (Eds.), Developments in Paleoenvironmental ResearchTracking Environmental Change Using Lake Sediments. Kluwer Academic Publishers, Dordrecht, pp. 171–203.
Appleby, P.G., Oldfield, F., 1978. The calculation of lead-210 dates assuming a constant rate of supply of unsupported 210Pb to the sediment. Catena 5, 1–8. https://doi.org/10.1016/S0341-8162(78)80002-2.
Aquino-López, M.A., Blaauw, M., Christen, J.A., Sanderson, N.K., 2018. Bayesian analysis of 210 Pb dating. J. Agric. Biol. Environ. Stat. 23, 317–333. https://doi.org/10.1007/s13253-018-0328-7.
Awerinzew, S., 1907. Über einige Süsswasser-Protozoen der Bäreninsel. Zool. Anz. 31, 243–247.
Balik, V., 1994. On the soil testate Amoebae Fauna (Protozoa: Rhizopoda) of the Spitsbergen Islands (Svalbard). Arch. fur Protistenkd. 144, 365–372. https://doi.org/10.1016/S0003-9365(11)80239-3.
Beyens, L., Bobrov, A., 2016. Evidence supporting the concept of a regionalized distribution of testate amoebae in the Arctic. Acta Protozool. 55, 197–209. https://doi.org/10.4467/16890027AP.16.019.6006.
Beyens, L., Chardez, D., 1995. An Annotated List of Testate Amoebae Observed in the Arctic between the Longitudes 27° E and 168° W. Arch. für Protistenkd. 146, 219–233. https://doi.org/10.1016/S0003-9365(11)80114-4.
Beyens, L., Chardez, D., 1987. Evidence from testate amoebae for changes in some local hydrological conditions between c. 5000 BP and c. 3800 BP on Edgeøya (Svalbard). Polar Res. 5, 165–169. https://doi.org/10.3402/polar.v5i2.6873.
Beyens, L., Chardez, D., De Bock, P., 1986a. Some new and rare testate amoebae from the Arctic. Acta Protozool. 25, 81–91.
Beyens, L., Chardez, D., De Landtsheer, R., De Baere, D., 1986b. Testate amoebae communities from aquatic habitats in the Arctic. Polar Biol. 6, 197–205. https://doi.org/10.1007/BF00443396.
Beyens, L., Chardez, D., De Landtsheer, R., De Bock, P., Jacques, E., 1986c. Testate amoebae populations from moss and lichen habitats in the Arctic. Polar Biol. 5, 165–173. https://doi.org/10.1007/BF00441696.
Bobrov, A.A., Wetterich, S., 2012. Testate amoebae of Arctic tundra landscapes. Protistology 7, 51–58.
Bonnet, L., 1965. Sur le peuplement thécamoebien de quelques sols du Spitsberg. Bull. la Société d'Histoire Nat. Toulouse 100, 281–293.
Booth, R.K., 2008. Testate amoebae as proxies for mean annual water-table depth in Sphagnum-dominated peatlands of North America. J. Quat. Sci. 23, 43–57. https://doi.org/10.1002/jqs.v23:110.1002/jqs.1114.
Booth, R.K., Lamentowicz, M., Charman, D.J., 2010. Preparation and analysis of testate amoebae in peatland palaeoenvironmental studies. Mires Peat 7, 1–7.
Bridgham, S.D., Pastor, J., Janssens, J.A., Chapin, C., Malterer, T.J., 1996. Multiple limiting gradients in peatlands: A call for a new paradigm. Wetlands 16, 45–65. https://doi.org/10.1007/BF03160645.
Chambers, F.M., Beilman, D.W., Yu, Z., 2011. Methods for determining peat humification and for quantifying peat bulk density, organic matter and carbon content for palaeostudies of climate and peatland carbon dynamics. Mires Peat 7, 1–10.
Chardez, D., Beyens, L., 1988. Centropyxis gasparella spnovand Parmulina louisi spnov., New Testate Amoebae from the Canadian High Arctic (Devon Island, NWT). Arch. fur Protistenkd. 136, 337–344. https://doi.org/10.1016/S0003-9365(88)80014-9.
Charman, D.J., Blundell, A., Abrupt Climate Change Over the European Land Mass project members, 2007. A new European testate amoebae transfer function for palaeohydrological reconstruction on ombrotrophic peatlands. J. Quat. Sci. 22, 209–221. https://doi.org/10.1002/jqs.1026.
Charman, D.J., Hendon, D., Woodland, W.A., 2000. The identification of testate amoebae (Protozoa: Rhizopoda) in peats: QRA Technical Guide No. 9, Quaternary Research Association. Quaternary Research Association, London. https://doi.org/10.1016/j.quascirev.2004.02.012.
Ehrenberg, C.G., 1870. Die Mikroskopischen Lebensverhaltnisse auf der Oberflache der Insel Spitzbergen. Monatber. Akad. Berlin 254–264.
Elvevold, S., Dallmann, W., Blomeier, D., 2007. Geology of Svalbard. Norwegian Polar Institute, Tromsø, Norway.
Evans, C.D., Peacock, M., Baird, A.J., Artz, R.R.E., Burden, A., Callaghan, N., Chapman, P.J., Cooper, H.M., Coyle, M., Craig, E., Cumming, A., Dixon, S., Gauci, V., Grayson, R.P., Helfter, C., Heppell, C.M., Holden, J., Jones, D.L., Kaduk, J., Levy, P., Matthews, R., McNamara, N.P., Misselbrook, T., Oakley, S., Page, S.E., Rayment, M., Ridley, L.M., Stanley, K.M., Williamson, J.L., Worrall, F., Morrison, R., 2021. Overriding water table control on managed peatland greenhouse gas emissions. Nature 593, 548–552. https://doi.org/10.1038/s41586-021-03523-1.
Førland, E.J., Benestad, R., Hanssen-Bauer, I., Haugen, J.E., Skaugen, T.E., 2011. Temperature and precipitation development at Svalbard 1900–2100. Adv. Meteorol. 2011, 1–14. https://doi.org/10.1155/2011/893790.
Gallego-Sala, A.V., Charman, D.J., Brewer, S., Page, S.E., Prentice, I.C., Friedlingstein, P., Moreton, S., Amesbury, M.J., Beilman, D.W., Björck, S., Blyakharchuk, T., Bochicchio, C., Booth, R.K., Bunbury, J., Camill, P., Carless, D., Chimner, R.A., Clifford, M., Cressey, E., Courtney-Mustaphi, C., De Vleeschouwer, F., de Jong, R., Fialkiewicz-Koziel, B., Finkelstein, S.A., Garneau, M., Githumbi, E., Hribjlan, J., Holmquist, J., Hughes, P.D.M., Jones, C., Jones, M.C., Karofeld, E., Klein, E.S., Kokfelt, U., Korhola, A., Lacourse, T., Le Roux, G., Lamentowicz, M., Large, D., Lavoie, M., Loisel, J., Mackay, H., MacDonald, G.M., Makila, M., Magnan, G., Marchant, R., Marcisz, K., Martínez Cortizas, A., Massa, C., Mathijssen, P., Mauquoy, D., Mighall, T., Mitchell, F.J.G., Moss, P., Nichols, J., Oksanen, P.O., Orme, L., Packalen, M.S., Robinson, S., Roland, T.P., Sanderson, N.K., Sannel, A.B.K., Silva-Sánchez, N., Steinberg, N., Swindles, G.T., Turner, T.E., Uglow, J., Väliranta, M., van Bellen, S., van der Linden, M., van Geel, B., Wang, G., Yu, Z., Zaragoza-Castells, J., Zhao, Y., 2018. Latitudinal limits to the predicted increase of the peatland carbon sink with warming. Nat. Clim. Chang. 8, 907–913. https://doi.org/10.1038/s41558-018-0271-1.
Gorham, E., Janssens, J.A., Wheeler, G.A., Glaser, P.H., 1987. The natural and anthropogenic acidification of peatlands. In: Hutchinson, T.C., Meema, K.M. (Eds.), Effects of Atmospheric Pollutants on Forests, Wetlands and Agricultural Ecosystems. NATO ASI Series (Series G: Ecological Sciences). Springer, Berlin Heidelberg, pp. 493–512. https://doi.org/10.1007/978-3-642-70874-9_36.
Hanssen-Bauer, I., Førland, E.J., Hisdal, H., Mayer, S., Sandø, A.B., Sorteberg, A., Adakudlu, M., Andresen, J., Bakke, J., Beldring, S., Benestad, R., Bilt, W., Bogen, J., Borstad, C., Breili, K., Breivik, Ø., Børsheim, K.Y., Christiansen, H.H., Dobler, A., Engeset, R., Frauenfelder, R., Gerland, S., Gjelten, H.M., Gundersen, J., Isaksen, K., Jaedicke, C., Kierulf, H., Kohler, J., Li, H., Lutz, J., Melvold, K., Mezghani, A., Nilsen, F., Nilsen, I.B., Nilsen, J.E.Ø., Pavlova, O., Ravndal, O., Risebrobakken, B., Saloranta, T., Sandven, S., Schuler, T.V., Simpson, M.J.R., Skogen, M., Smedsrud, L. H., Sund, M., Vikhamar-Schuler, D., Westermann, S., Wong, W.K., 2019. Climate in Svalbard 2100 - a knowledge base for climate adaptation. Norwegian Environment Agency (Miljødirektoratet).
Hugelius, G., Strauss, J., Zubrzycki, S., Harden, J.W., Schuur, E.A.G., Ping, C.-L., Schirrmeister, L., Grosse, G., Michaelson, G.J., Koven, C.D., O'Donnell, J.A., Elberling, B., Mishra, U., Camill, P., Yu, Z., Palmtag, J., Kuhry, P., 2014. Estimated stocks of circumpolar permafrost carbon with quantified uncertainty ranges and identified data gaps. Biogeosciences 11, 6573–6593. https://doi.org/10.5194/bg-11-6573-2014.
Hugelius, G., Tarnocai, C., Broll, G., Canadell, J.G., Kuhry, P., Swanson, D.K., 2013. Earth System Science Data The Northern Circumpolar Soil Carbon Database: spatially distributed datasets of soil coverage and soil carbon storage in the northern permafrost regions. Earth Syst. Sci. Data 5, 3–13. https://doi.org/10.5194/essd-5-3-2013.
Isaksson, E., Hermanson, M., Hicks, S., Igarashi, M., Kamiyama, K., Moore, J., Motoyama, H., Muir, D., Pohjola, V., Vaikmäe, R., van de Wal, R.S.W., Watanabe, O., 2003. Ice cores from Svalbard—useful archives of past climate and pollution history. Phys. Chem. Earth, Parts A/B/C 28, 1217–1228. https://doi.org/10.1016/j.pce:2003.08.053.
Juggins, S., 2020. rioja: Analysis of Quaternary Science Data. R package version 0.9-26.
Kellogg, L.E., Bridgham, S.D., 2003. Phosphorus retention and movement across an ombrotrophic-minerotrophic peatland gradient. Biogeochemistry 63, 299–315. https://doi.org/10.1023/A:1023387019765.
Koven, C.D., Schuur, E.A.G., Schädel, C., Bohn, T.J., Burke, E.J., Chen, G., Chen, X., Ciais, P., Grosse, G., Harden, J.W., Hayes, D.J., Hugelius, G., Jafarov, E.E., Krinner, G., Kuhry, P., Lawrence, D.M., MacDougall, A.H., Marchenko, S.S., McGuire, A.D., Natali, S.M., Nicolsky, D.J., Olefeldt, D., Peng, S., Romanovsky, V.E., Schaefer, K.M., Strauss, J., Treat, C.C., Turetsky, M., 2015. A simplified, data-constrained approach to estimate the permafrost carbon–climate feedback. Philos. Trans. R. Soc. A Math. Phys. Eng. Sci. 373, 20140423. https://doi.org/10.1098/rsta.2014.0423.
Lamarre, A., Magnan, G., Garneau, M., Boucher, É., 2013. A testate amoeba-based transfer function for paleohydrological reconstruction from boreal and subarctic peatlands in northeastern Canada. Quat. Int. 306, 88–96. https://doi.org/10.1016/J.QUAINT.2013.05.054.
Lamentowicz, M., Lamentowicz, Ł., Payne, R.J., 2013. Towards quantitative reconstruction of peatland nutrient status from fens. Holocene 23, 1661–1665. https://doi.org/10.1177/0959683613508162.
Lawrence, D.M., Koven, C.D., Swenson, S.C., Riley, W.J., Slater, A.G., 2015. Permafrost thaw and resulting soil moisture changes regulate projected high-latitude $CO_2$ and $CH_4$ emissions. Environ. Res. Lett. 10, 094011. https://doi.org/10.1088/1748-9326/10/9/094011.
Masson-Delmotte, V., Zhai, P., Pörtner, H.-O., Roberts, D., Skea, J., Shukla, P.R., Pirani, A., Moufouma-Okia, W., Péan, C., Pidcock, R., Connors, S., Matthews, J.B.R., Chen, Y., Zhou, X., Gomis, M.I., Lonnoy, E., Maycock, T., Tignor, M., Waterfield, T., 2018. Intergovernmental Panel on Climate Change, 2018: Summary for Policymakers, in: Global Warming of 1.5°C. An IPCC Special Report on the Impacts of Global Warming of 1.5°C above Pre-Industrial Levels and Related Global Greenhouse Gas Emission Pathways, in the Context of Strengthening the Global Response to the Threat of Climate Change,. pp. 3–24. https://doi.org/10.1017/CBO9781107415324.
Mazei, Y.A., Lebedeva, N.V., Taskaeva, A.A., Ivanovsky, A.A., Chernyshov, V.A., Tsyganov, A.N., Payne, R.J., 2018. Potential influence of birds on soil testate amoebae in the Arctic. Polar Sci. 16, 78–85. https://doi.org/10.1016/j.polar.2018.03.001.
Mitchell, E.A.D., 2004. Response of Testate Amoebae (Protozoa) to N and P Fertilization in an Arctic Wet Sedge Tundra. Arctic. Antarct. Alp. Res. 36, 78–83. https://doi.org/10.1657/1523-0430(2004)036[0078:ROTAPT]2.0.CO;2.
Nakatsubo, T., Uchida, M., Sasaki, A., Kondo, M., Yoshitake, S., Kanda, H., 2015. Carbon accumulation rate of peatland in the High Arctic, Svalbard: Implications for carbon sequestration. Polar Sci. 9, 267–275. https://doi.org/10.1016/j.polar.2014.12.002.

Norwegian Polar Institute, 2014. Terrengmodell Svalbard (S0 Terrengmodell, Svalbard-mosaikker). https://doi.org/https://doi.org/10.21334/npolar.2014.dce53a47.
Norwegian Polar Institute, 2014. Kartdata Svalbard 1:100 000 (S100 Kartdata, ESRI Shapefile). https://doi.org/https://doi.org/10.21334/npolar.2014.645336c7.
Nowak, A., Hodson, A., 2014. Changes in meltwater chemistry over a 20-year period following a thermal regime switch from polythermal to cold-based glaciation at Austre Brøggerbreen. Svalbard. Polar Res. 33, 22779. https://doi.org/10.3402/polar.v33.22779.
Oksanen, J., Blanchet, F.G., Friendly, M., Kindt, R., Legendre, P., McGlinn, D., Minchin, P.R., O'Hara, R.B., Simpson, G.L., Solymos, P., Stevens, M.H.H., Szoecs, E., Wagner, H., 2020. vegan: Community Ecology Package. R package version 2.5-7.
Olefeldt, D., Turetsky, M.R., Crill, P.M., McGuire, A.D., 2013. Environmental and physical controls on northern terrestrial methane emissions across permafrost zones. Glob. Chang. Biol. 19, 589–603. https://doi.org/10.1111/gcb.2012.19.issue-210.1111/gcb.12071.
Opravilova, V., 1989. Some Information on the Testate Amoebae from Spitsbergen. Fauna Norv. Ser. A10, 33–37.
Payne, R., 2007. Laboratory experiments on testate amoebae preservation in peats: implications for palaeoecology and future studies. Acta Protozool. 46, 325–332.
Payne, R.J., 2011. Can testate amoeba-based palaeohydrology be extended to fens? J. Quat. Sci. 26, 15–27. https://doi.org/10.1002/jqs.1412.
Payne, R.J., Kishaba, K., Blackford, J.J., Mitchell, E.A.D., 2006. Ecology of testate amoebae (protista) in south-central Alaska peatlands: Building transfer-function models for palaeoenvironmental studies. Holocene 16, 403–414. https://doi.org/10.1191/0959683606hl936rp.
Penard, E., 1903. Notice sur les rhizopodes du Spitsberg. Arch. für Protistenkd. 2, 238–282.
Qin, Y., Li, H., Mazei, Y., Kurina, I., Swindles, G.T., Bobrov, A., Tsyganov, A.N., Gu, Y., Huang, X., Xue, J., Lamentowicz, M., Marcisz, K., Roland, T., Payne, R.J., Mitchell, E.A.D., Xie, S., 2021. Developing a continental-scale testate amoeba hydrological transfer function for Asian peatlands. Quat. Sci. Rev. 258, 106868. https://doi.org/10.1016/j.quascirev.2021.106868.
R Core Team, 2020. R: a language and environment for statistical computing. Version 3.6.3.
Reimer, P.J., Austin, W.E.N., Bard, E., Bayliss, A., Blackwell, P.G., Bronk Ramsey, C., Butzin, M., Cheng, H., Edwards, R.L., Friedrich, M., Grootes, P.M., Guilderson, T.P., Hajdas, I., Heaton, T.J., Hogg, A.G., Hughen, K.A., Kromer, B., Manning, S.W., Muscheler, R., Palmer, J.G., Pearson, C., van der Plicht, J., Reimer, R.W., Richards, D.A., Scott, E.M., Southon, J.R., Turney, C.S.M., Wacker, L., Adolphi, F., Büntgen, U., Capano, M., Fahrni, S.M., Fogtmann-Schulz, A., Friedrich, R., Köhler, P., Kudsk, S., Miyake, F., Olsen, J., Reinig, F., Sakamoto, M., Sookdeo, A., Talamo, S., 2020. The IntCal20 Northern Hemisphere Radiocarbon Age Calibration Curve (0–55 cal kBP). Radiocarbon 62, 725–757. https://doi.org/10.1017/RDC.2020.41.
Schlegel, A., Lisker, F., Dörr, N., Jochmann, M., Schubert, K., Spiegel, C., 2013. Petrography and geochemistry of siliciclastic rocks from the Central Tertiary Basin of Svalbard - implications for provenance, tectonic setting and climate. Zeitschrift der Dtsch. Gesellschaft für Geowissenschaften 164, 173–186. https://doi.org/10.1127/1860-1804/2013/0012.
Schönborn, W., 1966. Beitrag zur Ökologie und Systematik der Testaceen Spitsbergens. Limnologica 4, 463–470.
Schuur, E.A.G., McGuire, A.D., Schädel, C., Grosse, G., Harden, J.W., Hayes, D.J., Hugelius, G., Koven, C.D., Kuhry, P., Lawrence, D.M., Natali, S.M., Olefeldt, D., Romanovsky, V.E., Schaefer, K., Turetsky, M.R., Treat, C.C., Vonk, J.E., 2015. Climate change and the permafrost carbon feedback. Nature 520, 171–179. https://doi.org/10.1038/nature14338.
Scourfield, D.J., 1897. Contributions to the non-marine fauna of Spitsbergen. Part I. Preliminary notes, and reports on the Rhizopoda, Tardigrada, Entomostraca, & c. Proc. Zool. Soc. London 65, 784–792.
Serreze, M.C., Barry, R.G., 2011. Processes and impacts of Arctic amplification: A research synthesis. Glob. Planet. Change 77, 85–96. https://doi.org/10.1016/j.gloplacha.2011.03.004.
Siemensma, F.J., 2021. Microworld, world of amoeboid organisms [WWW Document]. World-wide Electron. Publ. http://www.arcella.nl.
Sim, T.G., Swindles, G.T., Morris, P.J., Baird, A.J., Cooper, C.L., Gallego-Sala, A.V., Charman, D.J., Roland, T.P., Borken, W., Mullan, D.J., Aquino-López, M.A., Gałka, M., 2021. Divergent responses of permafrost peatlands to recent climate change. Environ. Res. Lett. 16, 034001. https://doi.org/10.1088/1748-9326/abe00b.
Sim, T.G., Swindles, G.T., Morris, P.J., Gałka, M., Mullan, D., Galloway, J.M., 2019. Pathways for ecological change in Canadian High Arctic wetlands under rapid twentieth century warming. Geophys. Res. Lett. 46, 4726–4737. https://doi.org/10.1029/2019GL082611.
Simpson, G.L., Oksanen, J., 2020. analogue: Analogue and Weighted Averaging Methods for Palaeoecology.
Swindles, G.T., Amesbury, M.J., Turner, T.E., Carrivick, J.L., Woulds, C., Raby, C., Mullan, D., Roland, T.P., Galloway, J.M., Parry, L., Kokfelt, U., Garneau, M., Charman, D.J., Holden, J., 2015. Evaluating the use of testate amoebae for palaeohydrological reconstruction in permafrost peatlands. Palaeogeogr. Palaeoclimatol. Palaeoecol. 424, 111–122. https://doi.org/10.1016/J.PALAEO.2015.02.004.
Swindles, G.T., Baird, A.J., Kilbride, E., Low, R., Lopez, O., 2018. Testing the relationship between testate amoeba community composition and environmental variables in a coastal tropical peatland. Ecol. Indic. 91, 636–644. https://doi.org/10.1016/j.ecolind.2018.03.021.
Swindles, G.T., Charman, D.J., Roe, H.M., Sansum, P.A., 2009. Environmental controls on peatland testate amoebae (Protozoa: Rhizopoda) in the North of Ireland: Implications for Holocene palaeoclimate studies. J. Paleolimnol. 42, 123–140. https://doi.org/10.1007/s10933-008-9266-7.
Swindles, G.T., Roe, H.M., 2007. Examining the dissolution characteristics of testate amoebae (Protozoa: Rhizopoda) in low pH conditions: Implications for peatland palaeoclimate studies. Palaeogeogr. Palaeoclimatol. Palaeoecol. 252, 486–496. https://doi.org/10.1016/j.palaeo.2007.05.004.
Swindles, G.T., Roland, T.P., Amesbury, M.J., Lamentowicz, M., McKeown, M.M., Sim, T.G., Fewster, R.E., Mitchell, E.A.D., 2020. Quantifying the effect of testate amoeba decomposition on peat-based water-table reconstructions. Eur. J. Protistol. 74, 125693. https://doi.org/10.1016/j.ejop.2020.125693.
Tanneberger, F., Tegetmeyer, C., Busse, S., Barthelmes, A., Shumka, S., Moles Mariné, A., Jenderedjian, K., Steiner, G.M., Essl, F., Etzold, J., Mendes, C., Kozulin, A., Frankard, P., Milanović, Đ., Ganeva, A., Apostolova, I., Alegro, A., Delipetrou, P., Navrátilová, J., Risager, M., Leivits, A., Fosaa, A.M., Tuominen, S., Muller, F., Bakuradze, T., Sommer, M., Christanis, K., Szurdoki, E., Oskarsson, H., Brink, S.H., Connolly, J., Bragazza, L., Martinelli, G., Aleksāns, O., Priede, A., Sungaila, D., Melovski, L., Belous, T., Saveljić, D., De Vries, F., Moen, A., Dembek, W., Mateus, J., Hanganu, J., Sirin, A., Markina, A., Napreenko, M., Lazarević, P., Stanová, V.Š., Skoberne, P., Heras Pérez, P., Pontevedra-Pombal, X., Lonnstad, J., Küchler, M., Wüst-Galley, C., Kirca, S., Mykytiuk, O., Lindsay, R., Joosten, H., 2017. The peatland map of Europe. Mires peat 19, 1–17. https://doi.org/10.19189/MaP.2016.OMB.264.
Taylor, L.S., Swindles, G.T., Morris, P.J., Gałka, M., 2019a. Ecology of peatland testate amoebae in the Alaskan continuous permafrost zone. Ecol. Indic. 96, 153–162. https://doi.org/10.1016/J.ECOLIND.2018.08.049.
Taylor, L.S., Swindles, G.T., Morris, P.J., Gałka, M., Green, S.M., 2019b. Evidence for ecosystem state shifts in Alaskan continuous permafrost peatlands in response to recent warming. Quat. Sci. Rev. 207, 134–144. https://doi.org/10.1016/j.quascirev.2019.02.001.
Tiner, R.W., 2016. Wetland Indicators: A Guide to Wetland Formation, Identification, Delineation, Classification, and Mapping, 2nd ed. Taylor & Francis, Boca Raton.
Väliranta, M., Salojärvi, N., Vuorsalo, A., Juutinen, S., Korhola, A., Luoto, M., Tuittila, E.-S., 2017. Holocene fen–bog transitions, current status in Finland and future perspectives. Holocene 27, 752–764. https://doi.org/10.1177/0959683616670471.
Vikhamar Schuler, T., Østby, T.I., 2020. Svalbard-Imp: A gridded forcing dataset for climate change impact research on Svalbard. Earth Syst. Sci. Data 12, 875–885. https://doi.org/10.5194/essd-12-875-2020.
Vitt, D.H., Chee, W.-L., 1990. The relationships of vegetation to surface water chemistry and peat chemistry in fens of Alberta, Canada. Vegetatio 89, 87–106. https://doi.org/10.1007/BF00032163.
Waddington, J.M., Morris, P.J., Kettridge, N., Granath, G., Thompson, D.K., Moore, P.A., 2015. Hydrological feedbacks in northern peatlands. Ecohydrology 8, 113–127. https://doi.org/10.1002/eco.v8.110.1002/eco.1493.
Walczowski, W., Piechura, J., 2011. Influence of the West Spitsbergen Current on the local climate. Int. J. Climatol. 31, 1088–1093. https://doi.org/10.1002/joc.2338.
Walker, D.A., Raynolds, M.K., Daniëls, F.J.A., Einarsson, E., Elvebakk, A., Gould, W.A., Katenin, A.E., Kholod, S.S., Markon, C.J., Melnikov, E.S., Moskalenko, N.G., Talbot, S.S., Yurtsev, B.A., The other members of the CAVM Team, 2005. The Circumpolar Arctic vegetation map. J. Veg. Sci. 16, 267–282. https://doi.org/10.1111/jvs.2005.16.issue-310.1111/j.1654-1103.2005.tb02365.x.
Warner, B.G., Rubec, C.D.A., 1997. The Canadian Wetland Classification System (Second Edition), 2nd ed. Wetlands Research Centre, Waterloo, Ontario, Canada.
Woo, M., Young, K.L., 2006. High Arctic wetlands: Their occurrence, hydrological characteristics and sustainability. J. Hydrol. 320, 432–450. https://doi.org/10.1016/j.jhydrol.2005.07.025.
Zhang, H., Amesbury, M.J., Ronkainen, T., Charman, D.J., Gallego-Sala, A.V., VÄliranta, M., 2017. Testate amoeba as palaeohydrological indicators in the permafrost peatlands of north-east European Russia and Finnish Lapland. J. Quat. Sci. 32, 976–988. https://doi.org/10.1002/jqs.v32.710.1002/jqs.2970.